nuclear technology/Fusion

AUTHORS — OCTOBER 1982

FUSION REACTORS

STUDIES OF THE PHYSICS AND ENGINEERING OF DEUTERIUM-DEUTERIUM BARRIER TANDEM MIRROR REACTORS

R. W. Conn
V. K. Dhir
N. M. Ghoniem
D. M. Goebel
S. P. Grotz
F. Kantrowitz
N. S. Kim
T. K. Mau
G. W. Shuy
M. Z. Youssef

R. W. Conn (front row, middle) (PhD, California Institute of Technology, 1968) is currently a professor of engineering and applied science at the University of California–Los Angeles (UCLA). **V. K. Dhir** (not pictured) (PhD, Kentucky University, 1972) is currently a professor of engineering and applied science at UCLA. **N. M. Ghoniem** (front row, right) (PhD, University of Wisconsin, 1977) is currently an associate professor of engineering and applied science at UCLA. **D. M. Goebel** (back row, second from left) (PhD, UCLA, 1981) is currently an associate development engineer in the Fusion Engineering and Physics Program at UCLA and a technical staff member in the Energy Technology Division at TRW, Inc. **S. P. Grotz** (back row, far right) (BS, University of Wisconsin, 1979) is an assistant development engineer in the Fusion Engineering and Physics Program at UCLA. **F. Kantrowitz** (back row, far left) is currently working on his PhD at UCLA. **N. S. Kim** (back row, second from right) (PhD, Brown University, 1978) is an assistant research engineer in the Fusion Engineering and Physics Program at UCLA. **T. K. Mau** (not pictured) (PhD, University of Wisconsin, 1977) is an assistant research engineer in the Fusion Engineering and Physics Program at UCLA. **G. W. Shuy** (not pictured) (PhD, University of Wisconsin, 1980) is an assistant research engineer in the Fusion Engineering and Physics Program at UCLA. **M. Z. Youssef** (front row, left) (PhD, University of Wisconsin, 1980) is an assistant research engineer in the Fusion Engineering and Physics Program at UCLA.

PLASMA ENGINEERING

PARTIALLY CATALYZED DEUTERIUM AND TRITIUM-ASSISTED PLASMA CHARACTERISTICS

Ehud Greenspan
George H. Miley

Ehud Greenspan (right) (BSc, mechanical engineering, Technion; PhD, nuclear science and engineering, Cornell University) was a visiting professor in the Nuclear Engineering Program of the University of Illinois from 1979 to 1981, on leave from the Nuclear Research Center and the Ben-Gurion University of the Negev, Israel. He held visiting appointments at the Princeton

32

9W

FUSION REACTORS

STUDIES OF THE PHYSICS AND ENGINEERING OF DEUTERIUM-DEUTERIUM BARRIER TANDEM MIRROR REACTORS

R. W. CONN, V. K. DHIR, N. M. GHONIEM, D. M. GOEBEL, S. P. GROTZ, F. KANTROWITZ, N. S. KIM, T. K. MAU, G. W. SHUY, and M. Z. YOUSSEF
University of California, Los Angeles
School of Engineering and Applied Science, Los Angeles, California 90024

Received October 15, 1981
Accepted for Publication May 5, 1982

A study of barrier tandem mirrors as deuterium-deuterium (D-D) cycle reactors shows that high central cell beta and axisymmetry are crucial to even a moderate Q reactor. The SATYR system is large, with low-power density, and Q ~ 5 to 6. A specialized axisymmetric configuration involving a plug-barrier cell with a levitated internal ring has been developed, though overall results are independent of the specific axisymmetric end plug configuration. The internal ring thermal analysis, including both surface and neutron volumetric heating, revealed unexpectedly that the operating time between recooling periods is limited by the time to reach the temperature limit of the superinsulator rather than the time for the superconductor to reach some predetermined level (e.g., 12 K for Nb-Ti). Further, it is found that a melt-layer within the ring is not required. A new pressure-vessel-type blanket design with pebble beds of ferritic steel produces high blanket multiplication and has long life (exceeding plant life). The overall study is presented along with detailed analyses in problem topics ranging from reactor physics on the one hand to detailed fusion engineering on the other. Specific subjects analyzed include reactor plasma performance, magnetic configuration development, coil design, blanket nuclear analysis and thermal hydraulics, blanket materials, structural analyses, and lifetime. A detailed comparison of economic, environmental, and safety scaling factors for D-D and deuterium-tritium (D-T) reactors reveals few incentives for aiming at D-D devices. It is concluded that the linearity of tandem mirrors, their inherent modularity and potential for steady-state operation, their predicted high-power density and high Q value, combined with the findings of this study, suggest that optimized D-T-cycle barrier tandem mirror reactors with axisymmetry and high β_c have the potential to be economic reactor systems and should remain the major goal of mirror fusion research.

I. INTRODUCTION

The addition of a thermal barrier to separate electrons in a tandem mirror has been shown in theory[1] to permit high values of Q (the ratio of fusion power to total plasma input power) in deuterium-tritium (D-T) reactors. If central cell beta values can be high (~40%), moderate levels of neutral injection energy, electron heating power, peak magnetic field strength, and overall system size are predicted.[1-5] Estimated values for end loss $n\tau$ are high enough and scale in a manner that makes it interesting to examine deuterium-deuterium (D-D) cycle barrier tandem mirror reactors (BTMRs). Furthermore, it is well known that mirror end losses can in principle be efficiently (>50%) converted to electricity.[6] Since the D-D cycle produces more energy in charged particles relative to that in neutrons than the D-T cycle, and since end loss direct conversion is more efficient than thermal energy conversion, a D-D-based reactor can have a lower plasma Q value when the overall plant net electrical efficiency is the same as that in a D-T machine.[7]

Given these factors and the other commonly

touted advantages of D-D-cycle reactors,[8] it is of interest to develop a reasonably self-consistent D-D-based BTMR system, assess its practical feasibility, and compare it with the results of D-T-based BTMR studies.[1-5] This we have done in a study[9] referred to as "SATYR." In this paper, we present the overall study itself, from physics on the one hand to fusion engineering analysis on the other; report on major findings and conclusions; and discuss comparisons to D-T systems. Where appropriate, our findings are also compared with those from a recent D-D-based tokamak study,[10] which, in turn, was developed for comparative purposes as an extension of the STARFIRE D-T tokamak reactor design.[11]

II. THE SATYR STUDY

The objectives of the SATYR study are to assess the technical potential of barrier tandem mirrors as D-D-based reactors, to identify and analyze requirements and constraints imposed by the D-D fuel cycle choice, to advance generic reactor subsystem concepts (for example, steady-state blanket design), and to take advantage where feasible of the low-power density inherent to the D-D cycle. Related to the last point, we find for example that the predicted lifetime for first-wall and blanket components exceeds plant life (30 yr), a result that is important to plant economics, safety, and reliability. Of course the advantages to be derived from this result are difficult to quantify without a very detailed assessment of maintenance costs, reliability, and the offsetting effect of initially higher capital costs for a low-power density plant.

An initial assessment of D-D BTMR physics shows that the central cell beta value, β_c, should be >40% (we use 60% in SATYR). Earlier calculations of magnetohydrodynamic (MHD) ballooning modes indicate the limit for β_c is 20% or less for quadrupole stabilized configurations.[12] Recent work[13] on kinetic effects shows that higher β_c limits are likely but it remains a problem as to whether or not values much above 40% will be possible.

Fully axisymmetric plug-barrier configurations can be expected to have a higher limiting value for β_c. In addition, an axisymmetric plug-barrier-central-cell should eliminate neoclassical and resonant radial transport, as analyzed by Ryutov and Stupakov.[14] This is crucial for D-D-based reactors because a large central cell $n\tau$ value is required and any significant radial transport loss in addition to end loss is intolerable. Partially axisymmetric configurations have been developed to eliminate Ryutov-Stupakov transport but they still use a quadrupole for MHD stability.[15] Only the cusp configuration proposed by Logan[16] is fully axisymmetric. Because of its importance to D-D-based tandems, we have devoted considerable attention to the matter of axisymmetric configuration development. We have settled on an approach for SATYR but it is crucial to note that neither we nor other groups have yet developed a configuration attractive from a physics and engineering standpoint. Invention is still required.

II.A. Axisymmetric BTMR Configurations

Two possibly fully axisymmetric configurations have been considered in detail. Each configuration is axisymmetric along its full length and has an MHD stable barrier cell. The first design[17] is based on the large, axisymmetric mirror experiment (LAMEX) in which surface magnetic fields generated with SURMAC coils[18] are used to stabilize a simple mirror (see Fig. 1). The second configuration[19] (see Fig. 2) has the magnetic flux divided into two categories: the private flux, which encircles an internal coil, and the common flux, which maps into the central cell. The common flux region forms the plug and barrier. External trimming coils near the internal ring create a maximum in the field, which extends over the entire region of bad curvature in this area. A coil can be added between the plug-throat coil and the direct converter, creating an electrostatic potential auxiliary cell (or "A-cell") to plug particles leaking through the null points.

We first considered high mirror ratio ($R_m > 20$) LAMEX plugs in which the plug electron temperature is raised above the central cell electron temperature without the use of thermal barriers (as suggested by Wong[20]). This idea has been discarded because of particle leakage due to null scattering and the large plug volume. We examined LAMEX-type configurations as plugs with lower mirror ratio ($R_m \simeq 3$ to 4) and with a separate mirror cell as a barrier. The small circular throat allows a shorter, high mirror ratio barrier, which greatly improves reactor power balance and makes feasible the Q value of five or greater necessary in a D-D reactor. This, however, requires very high surface magnetic fields ($B_s = 8$ T) and beta values ($\beta_s \simeq 60\%$) and results in a "cramped" configuration with little room for shielding of the internal rings.

Finally, we consider a barrier based on LAMEX with a simple plug. This is a more "natural" way to use LAMEX since a high barrier mirror ratio raises the barrier potential drop, ϕ_b, and lowers the rate at which passing ions trap. There now exists a stabilized barrier directly connected to the central cell. Surface fields can be much lower ($B_s \simeq 1.5$ T) and beta values (~10%) are comparable to those observed in multipole experiments[21] and predicted by theory.[22] Since the barrier is much longer than the plug, and coils have a smaller cross section due to lower fields, there is now adequate room for shielding. The high barrier mirror ratio ($R_b = 20$) leads to good power balance characteristics for low plug beta.

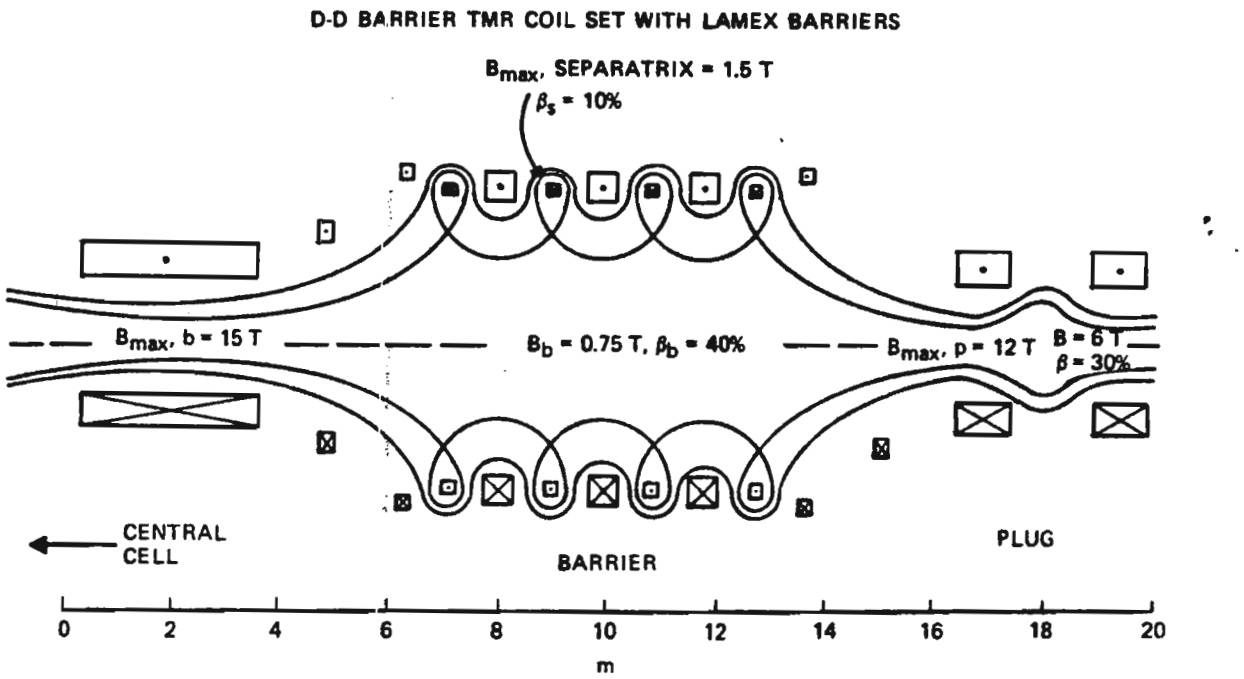

Fig. 1. View of right end barrier-plug arrangement for a tandem mirror utilizing an axisymmetric plug and barrier. The barrier is stabilized by the surface fields of the internal rings, following the approach of LAMEX experiments.

There are two problems with LAMEX tandem configurations that have led us to examine the single-ring configuration of Fig. 2. The first difficulty is the existence of off-axis nulls, which cause additional trapping of particles by null scattering due to lack of adiabaticity. An estimate[9] of the power required to offset this trapping is 300 MW, clearly too large. The second difficulty is that the pump beam must be placed along the field lines at the thermal barrier. This is very difficult to do in the surface field region yet 35 to 45% of the central cell flux maps into the surface region.

In the single-ring, field-reversed (SRFR) configuration (see Fig. 2), ions trapped in the plug or the barrier are only in regions of good field line curvature accomplished by creating a broad, flat maximum-field region extending completely through the bad curvature bridge region at the back of the coils. The existence of nulls in the magnetic field presents problems for single-particle confinement as well as MHD stability for plug and barrier ions. On the one hand, the motion of an ion in the vicinity of the null point is clearly nonadiabatic. On the other hand, it seems difficult to attain an MHD stable configuration by allowing the plasma pressure to peak away from the null. Fortunately, the nulls are on-axis and the axisymmetry of the system implies conservation of the canonical angular momentum for axis-encircling particles with trajectories arbitrarily close to the null points. This forms an effective potential well, which confines particles near the null. It is expected that plug and barrier ions will consist of axis-encircling particles in the common flux region near nulls, together with particles that are mirror trapped in the common flux region on field lines sufficiently far from the separatrix to ensure the adiabaticity of their motion. A coil can be added in between the plug throat coil and the direct converter, creating an electrostatic potential A-cell to plug particles leaking through the null points. Particles that are trapped in the private flux region do not perform any plugging function, nor do they provide added MHD stability. Their existence is a consequence of collisional transport and allows the radial pressure profile to peak on the separatrix, which maps to the center of the central cell. It should only be necessary for the private flux plasma to be a few ion Larmor radii thick.

Pumping the barrier requires a neutral beam with energy greater than $e\phi_b$ that is oriented along barrier field lines. Here, ϕ_b is the barrier potential. Since pumping power is inversely proportional to barrier mirror ratio, R_b, it is desirable to have a large value of R_b. However, if the barrier is not itself MHD stable, Newcomb and Pearlstein[23] have shown that a large mirror ratio will reduce the beta limit. With a stable, high mirror ratio barrier, a high beta limit ($\geq$40%) and high reactor Q ($P_{fusion}/P_{injection}$) should be possible.

One of the greatest assets of this configuration is its flexibility. If sloshing ions[24] or sloshing electrons[25] are used on the central cell side of the internal

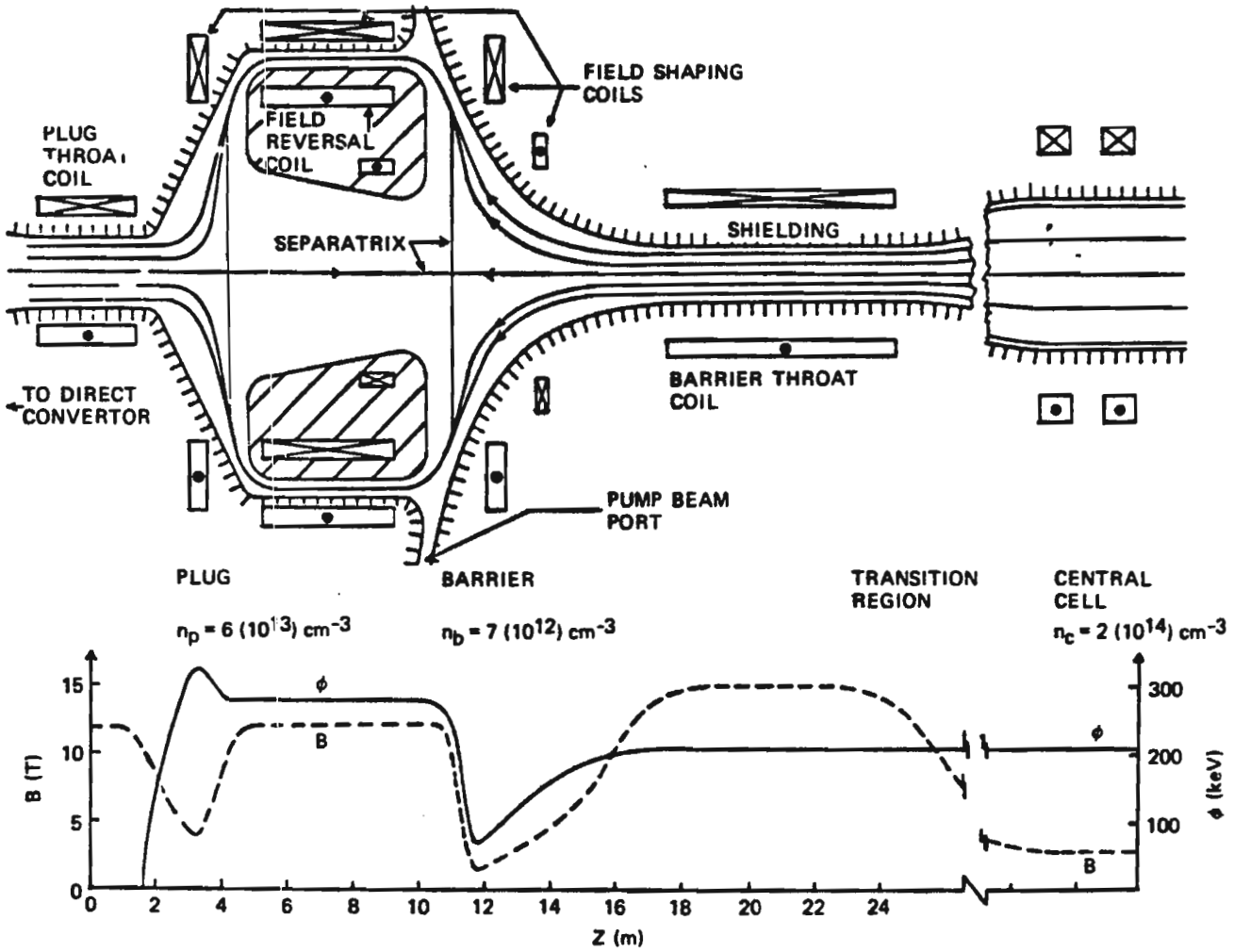

Fig. 2. View of the left end of a barrier-plug arrangement for a tandem mirror in which a single internal ring is used to reverse the field. The field variation for a separate barrier-plug cell arrangement is shown.

coil, both the plug and the barrier can be formed there, and the outer mirror becomes an A-cell. If the plug throat cell is eliminated, an annular plasma direct converter can be connected to the field-reversal coil, and the field-reversal coil can therefore be supported externally. If the barrier throat coil is eliminated, a configuration is created where both the central cell and the plug/barrier are MHD stable. Here the internal coil is open to the central cell, so neutron heating would be prohibitive in a D-T reactor. This may, however, be suitable for advanced fuels.

Although uncertain, we have chosen the SRFR configuration as the basis for the SATYR study. This has led us to examine the MHD of the configuration along with engineering questions such as the design of a levitated internal ring, including its shielding, and the possibility of using current and coolant leads for the hoops. The remainder of our work is generic to any axisymmetric BTMR. Our results on physics performance requirements, and engineering, plant design, and system characteristics (particularly as compared to D-T-based systems) are generally applicable.

II.B. Reactor Plasma Analysis

In the current SATYR design, negative field-line curvature in the transition region between the central cell solenoid and the thermal barrier can drive ballooning interchange modes. The ballooning instability then effectively limits the attainable values of the central cell β even when high β stable plugs or barrier are used. Thus it is important to determine the relationship between central cell and plug β values for which a given field line is MHD stable. Optimization of the magnetic configuration[9] is performed using a code[26] obtained from Lawrence Livermore National Laboratory (LLNL). The net results for the central cell ballooning β_c limits are shown in Fig. 3. Values up to 60% are obtained for stabilizing plug

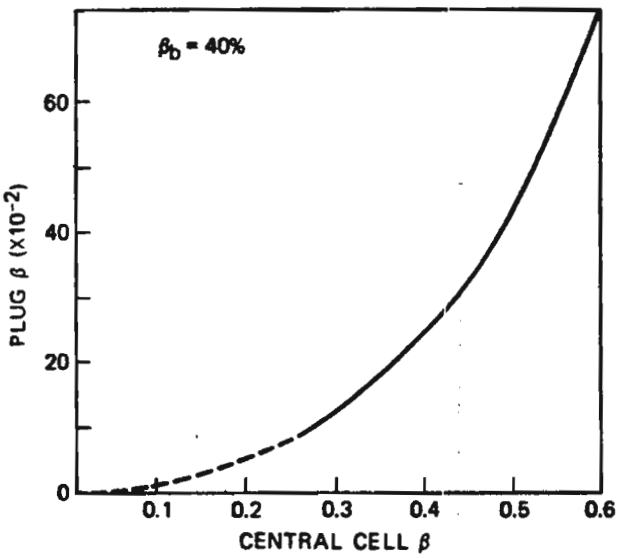

Fig. 3. Maximum central cell beta as a function of plug beta assuming the barrier beta is 40%. The result is for the SRFR end plug arrangement.

β values from 0 to 75% at a fixed value of β in the barrier (40%).

Reactor parameters have been computed using a modified version of a zero-dimensional equilibrium BTMR plasma power balance code developed by Santarius and Conn[4] and approximately modified for the peculiarities of the D-D cycle. Furthermore, effects associated with nuclear elastic scattering have been included[27]; i.e., that charged fusion products give more energy to ions, rather than assuming only Coulomb scattering governs slowing down and that the fuel ion distribution function gives a higher reactivity for a given ion temperature. Results are presented for the case of no nuclear scattering and when the reactivity is increased 25%. (This is probably the maximum such an effect can have. The two results show the range in which the true result will lie.)

A list of key parameters for SATYR is given in Table I along with parameters calculated for a D-T version of the SRFR configuration and parameters from the WITAMIR-I D-T reactor study.[5] We discuss a comparison of D-D and D-T reactors in Sec. III. It is clear however that the inherently low-power density of the D-D cycle leads to physically large reactors for a given level of output power. High β_c is critical in this regard. Lower values than 60% would mean even larger reactors. Concomitantly, the surface heat load and the neutron wall loading are both low, which will mean longer first-wall and blanket lifetime. The modest Q value (between 4.8 and 6.5 depending on various factors) means there will be a substantial (47%) recirculating power fraction in SATYR.

Various levels of plasma heating and type are required for SATYR. Most of the neutral beam power (75 MW per barrier cell) is required at 290 keV while 1.1 MW of very high energy (700-eV) beams are needed per plug. Negative ion sources are thus necessary but not available at the parameter levels required. The needed advances include:

1. a continuous source of 5 to 10 A of deuterium negative ions
2. a high voltage, continuously operating, negative ion accelerator
3. a continuously operating, high-speed pumping system
4. associated high-voltage power supplies for negative ion systems.

Not one of these items is available at this time, and it should be noted that a similar list was compiled 4 yr ago. Long pulse, 1- to 2-A negative ion beams have been required since then, but only just recently. Currents of 5 to 10 A per source might become available in a few years.

Electron heating using electron cyclotron resonance heating (ECRH) is required to heat plug electrons and raise their temperature, T_{ep}, above that of central cell electrons. In addition, since application of ECRH raises the perpendicular energy of the electrons, the barrier potential, ϕ_b, separating plug and central cell electrons can be enhanced by using ECRH to increase the density of hot barrier-trapped electrons. The impact of barrier ECRH is seen immediately upon examination of the expression

$$\phi_b = T_{ec} \ln\left(\frac{n_c}{n_b - n_{eh}}\right) ,$$

where n_c and n_b are the central cell and barrier plasma density, respectively, and n_{eh} is the hot barrier-trapped electron density.

We find[9] that launching and propagating ECRH microwave power into the plasma does not seem to pose serious problems. The exact location and orientation of the radiating antenna and the optimum wave parameters can be obtained using a ray-tracing technique to follow the microwave beam trajectories within the plasma. The absorption scenario is modified considerably from the warm plasma picture due to the several hundred kiloelectron volt temperature in the plasma. The theory of strongly relativistic electron absorption[28] needs to be fully developed before the wave deposition profile can be obtained. In general, strong absorption of the wave energy is anticipated with a shift in the peak absorption region and a spread in the heating profile.

Based on present-day technology for high-power microwave production, transmission, and radiation, the components of an ECRH system are identified

TABLE I

Parameters of the D-D Cycle SATYR and D-T Cycle Reactors

	SATYR D-D Cycle	Single-Ring Axisymmetric Tandem Mirror Reactor (TMR) D-T Cycle	WITAMIR-I[a] D-T Cycle
A. Power Parameters			
Q	6.5	32	28
Fusion power (MW)	2000	2000	3000
Injected power absorbed in plasma (MW)	308	62.5	107
Blanket thermal power (MW) (Neutron energy multiplication = 1.9 for D-D, 1.2 for D-T, except for WITAMIR-I)	1650	1930	3317
Power to direct converter (MW)	1345	450	502
Gross electric power (MW) ($\eta_{DC} = 0.6, \eta_{th} = 0.4$)	1625	1100	1860
Injected power (MW) ($\eta_{inj} = 0.5$)	625	130	246
Plug neutral beam trapping fraction	0.2	0.5	0.13
Auxiliary power (MW)	100	50	84
Net electric power (MW)	900	920	1530
Recirculating power fraction	0.47	0.16	0.18
Net efficiency	0.27	0.38	0.39
Neutral wall loading (MW/m^2)	0.41	3.2	2.4
At 14 MeV	0.35	3.2	2.4
At 2.45 MeV	0.06	0.003	---
Central cell surface heat load (MW/m^2)	0.13	0.035	0.020
Plug surface heat load (MW/m^2)	0.45	0.011	0.030
Barrier surface heat load (MW/m^2)	0.25	0.17	0.5
Fusion power density (MW/m^3)	2.2	15	11.3
B. Size and Magnetic Field Parameters			
Central cell length (m)	225	80	165
Plug and barrier total axial length, each end (m)	18	18	21
Total length, without direct converter (m)	261	116	207
Central cell magnetic field (T)	4	3	3.6
Barrier maximum field (T)	15	15	14
Barrier minimum field (T)	1.5	1.5	1.4
Plug maximum field (T)	12	9	6
Plug minimum field (T)	4.5	4	4
Vacuum mirror ratios			
Central cell	3.75	5	3.89
Barrier			
For passing ion density	10	10	10
For hot electron confinement	8	6	4.28
Plug	2.67	2.25	1.50
C. Plug Plasma Parameters			
Neutral beam injection energy (keV)	700	300	500
Average ion energy (keV)	1450	460	905
Electron temperature (keV)	290	75	123
Average density (m^{-3})	2.5×10^{19}	6.5×10^{19}	2.7×10^{19}
Potential $\phi_c + \phi_e$ (keV)	675	325	326
$(n\tau)_{ip}$ (m^{-3}·s)	4.5×10^{20}	8.8×10^{19}	9.8×10^{19}

[a]From Ref. 5.

(Continued)

TABLE I (Continued)

	SATYR D-D Cycle	Single-Ring Axisymmetric Tandem Mirror Reactor (TMR) D-T Cycle	WITAMIR-I[a] D-T Cycle
C. Plug Plasma Parameters (Continued)			
β_p	0.8	0.8	0.64
Neutral beam power absorbed, per plug (MW)	1.1	3.2	1.2
ECRH power absorbed, per plug (MW)	29	7.5	8.2
ECRH frequency, ω_{ce} (GHz)	56	50	67
Plasma radius (m)	1.18	0.69	0.77
D. Central Cell Plasma Parameters			
Average density (m^{-3})	2.1×10^{20}	1.7×10^{20}	1.51×10^{20}
Ion temperature (keV)	60	40	32.5
Electron temperature (keV)	57	32	32.8
$(n\tau)_{ic}$ ($m^{-3} \cdot s$)	5.2×10^{21}	7.6×10^{20}	7.8×10^{20}
β_c	0.7	0.7	0.4
Electron confining potential, ϕ_e (keV)	440	210	224
Ion confining potential, ϕ_c (keV)	235	115	102
Plasma radius (m)	1.14	0.72	0.72
E. Barrier Plasma Parameters			
Minimum density (m^{-3})	8.3×10^{18}	7.2×10^{18}	6.9×10^{18}
Pumping parameter, g_b	2	2	2
Potential, ϕ_b (keV)	270	160	141
Cold passing electron fraction, F_{ec}	0.20	0.13	0.27
Average hot electron energy	420	440	270
Potential well length (m)	6	6	10
Maximum plasma radius (m)	1.56	0.86	1.08
β_b	0.4	0.4	0.235
ECRH power absorbed, per barrier (MW)	25	8.5	16.7
ECRH frequency, ω_{ce} (GHz)	32.5	32.5	40
High energy pump neutral beams			
Energy (keV)	290	170	190
$\langle\sigma v\rangle_{cx}/\langle\sigma v\rangle_{ion}$	0.10	0.27	---
Power per barrier (MW)	75	8	21.2
Pumping fraction	0.05	0.05	0.05
Low energy pump neutral beams			
Energy (keV)	30	17	9.6
$\langle\sigma v\rangle_{cx}/\langle\sigma v\rangle_{ion}$	1.2	2.6	---
Power per barrier (MW)	25	4.4	6.4
Pumping fraction	0.95	0.95	0.95

[a]From Ref. 5.

for a preliminary base design. The components and their parameters are given in Table II. There is great economic incentive for reducing the number of microwave components by upgrading the power rating of each component by a factor of ~5.

II.C. Magnet Systems

The magnet arrangement for SATYR is shown in Fig. 4, and the magnetic field strength along the plasma surface is shown in Fig. 5. The magnets are all solenoids but fall in the following categories: (a) discrete central cell coils (53), (b) barrier coils (1 + 1), (c) internal field-reversal coils (1 + 1), (d) plug coils (1 + 1), and (e) trim coils (4 + 4). The central cell coil system, which is a series of discrete short solenoids, has an inside coil radius of 2.75 m. The centerline field is 4 T with a maximum field ripple of <5%. This can be lowered by adjusting the coil spacing. A niobium-titanium superconductor

TABLE II

Components of ECRH Microwave System*

	Plug	Barrier
A. Source—Gyrotron		
Output power (kW)	200	200
Frequency (GHz)	56	32.5
Efficiency (%)	~50	~50
Number per plug/barrier	150	130
B. Transmission System—Circular Waveguide		
Mode or propagation	TE_{01} (circular)	TE_{01} (circular)
Inner diameter (cm)	6	6
Power rating per line (kW)	200	200
Material	Copper or copper-coated aluminum	Copper or copper-coated aluminum
Attenuation (dB/km)	0.66	1.6
Length (m)	≲10	≲10
Number per plug	15	13
Pressure (atm)	~1	1
Filling gas	To be determined	To be determined
Coolant for wall	To be determined	To be determined
Window	To be determined	To be determined
Number of miter bends	~1 (90 deg)	~1 (90 deg)
Fractional power loss per unit (%)	~9	~4
C. Radiating System—Waveguide Aperture		
Radiating mode	TE_{11} (circular)	TE_{11} (circular)
Mode transducer	$TE_{01} \rightarrow TE_{11}$	$TE_{01} \rightarrow TE_{11}$
Transducer loss (dB)	>0.3	>0.3
Coupling (%)	>90	>90

*The components listed are those of a base system for a D-D-burning TMR. Since data on high-power, oversized waveguide propagation are lacking, some of the numbers quoted in the table are, at best, order of magnitude estimates. As such, the system design should be viewed as preliminary in nature rather than definitive.

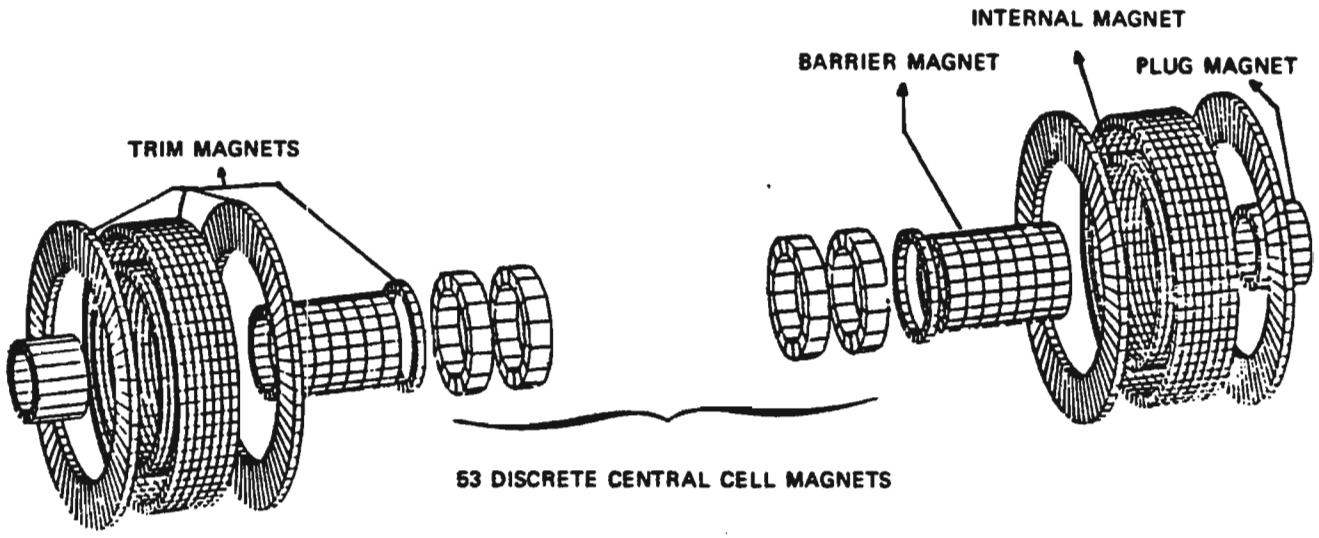

Fig. 4. Perspective view of the coil systems in SATYR.

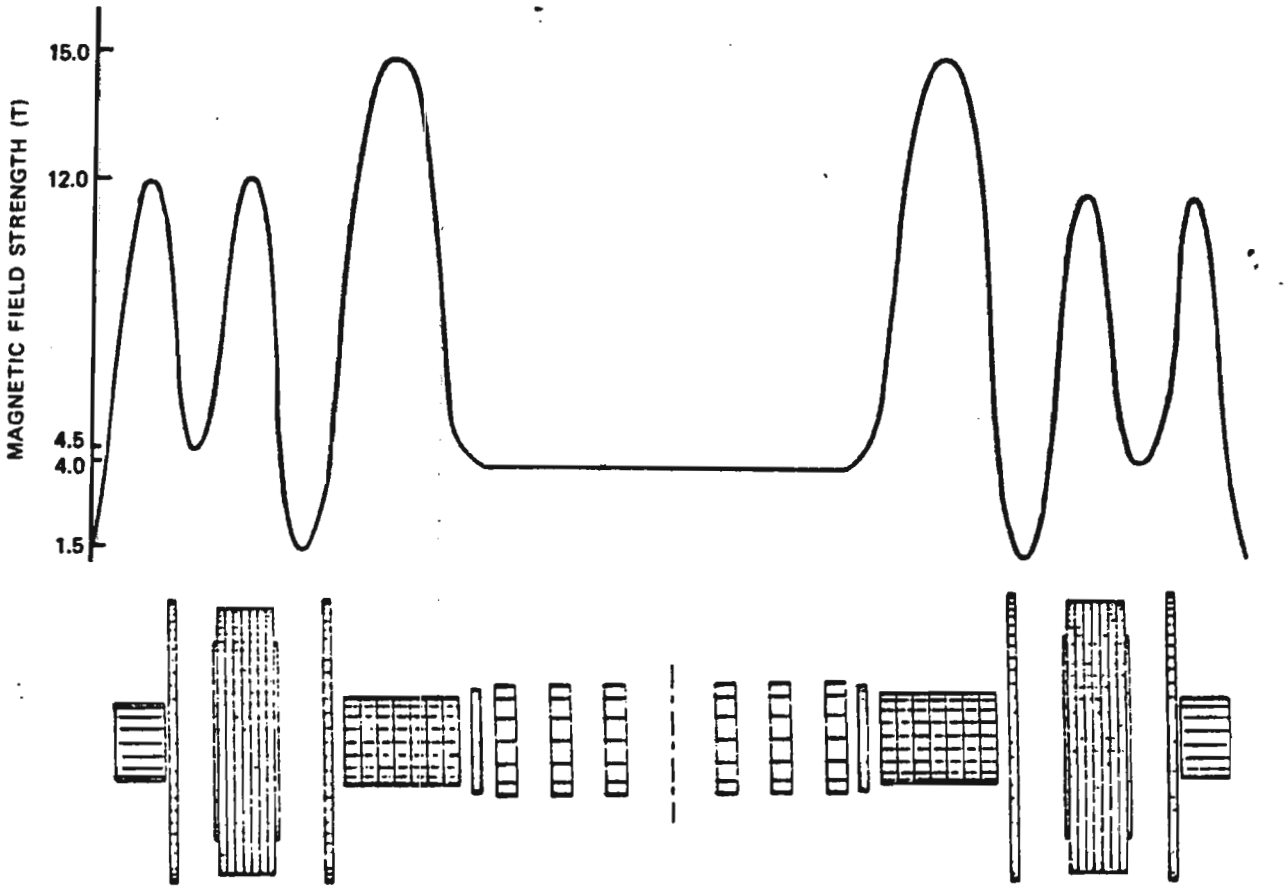

Fig. 5. Magnetic field variation along the centerline in SATYR.

will be used. Since the centerline field in the barrier coil requires 15 T, the barrier coil must have very high magnetic efficiency (~95%). Niobium-tin is the appropriate superconducting material. The length, the radial thickness, and the inner radius of the barrier coil are 5.0, 0.52, and 2.04 m, respectively. The plug coil is 4.0 m in length and has a 0.5-m radial thickness. The inside radius is 2.25 m and the centerline field strength is 12 T. Niobium-titanium is the superconductor.

While these coils represent a technical challenge, they would pose no serious impediment to implementing SATYR. The internal field-reversal coil is the major concern in the entire magnet system. It must produce a peak field of 12 T at a point ~0.5 m outside the magnet surface. It is a solenoid with an inside radius of 3.35 m, an axial length of 4.0 m, and a radial thickness of 0.9 m. Overall parameters for the internal ring are listed in Table III.

The following problems are faced when designing such a coil:

1. For plasma physics reasons, the magnetic field strength (12 T) just outside the magnetic surface must be homogeneous axially throughout the 4-m length. Uniform current density solenoids cannot generate such field homogeneity. A nonuniform current density solenoid design has been developed by dividing the coil axially into several sub-cross sections with different current densities. The outermost sub-cross section decreases toward the center of the coil.

2. Space for neutron shielding of the coil must be properly designed.

3. The cooling system must be special because, although the entire coil is cooled down with ordinary liquid helium, the transfer mechanism must be properly designed with the coil in the levitated position.

The internal ring is not subject to a large neutron loading because it is separated from the central cell by the barrier coil and its associated shielding. Nevertheless, the coil will be subject to some neutron and gamma heating from a source that is not uniform poloidally about the ring itself. A very detailed initial two-dimensional neutronics calculation was performed using the model system outlined in Fig. 6. Shielding is not uniform about the ring to save weight and because neutrons born in the central cell are

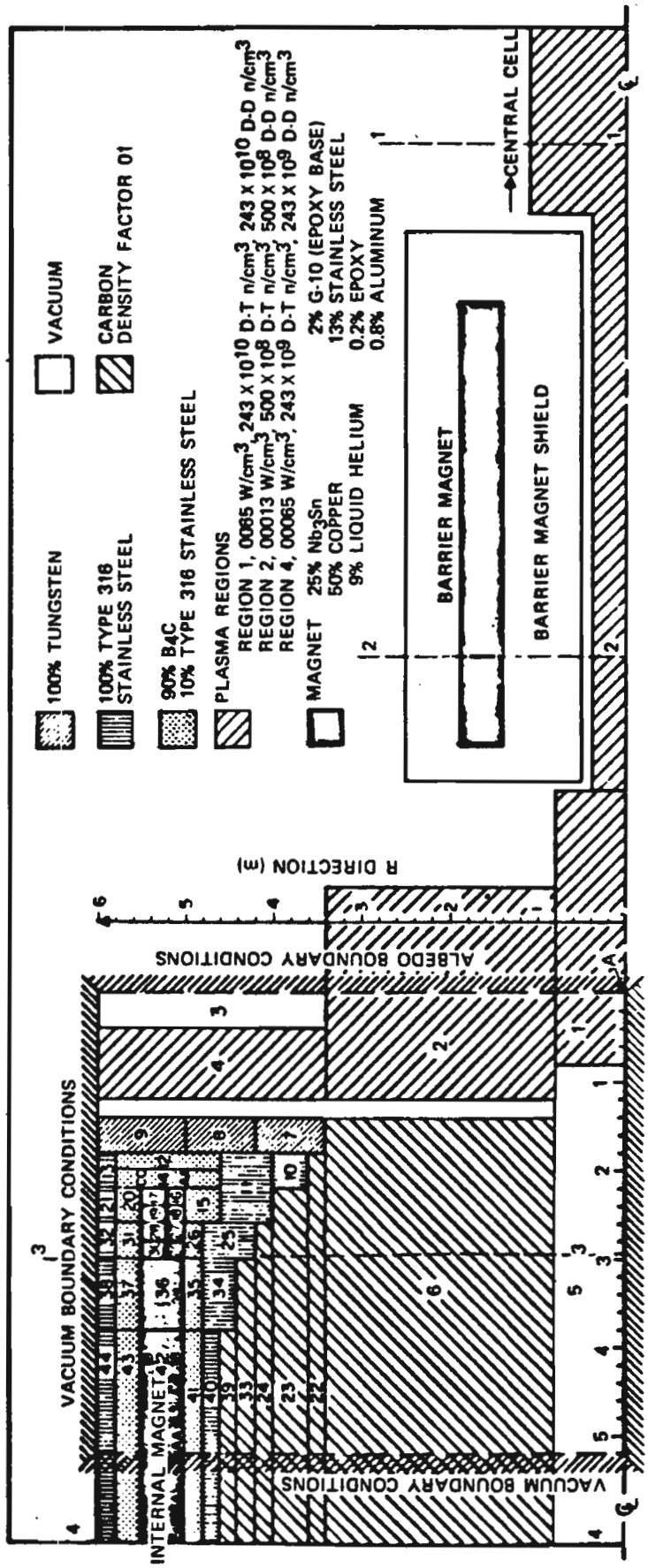

Fig. 6. Detailed geometric model of the barrier magnet, internal ring, and associated shielding used for two-dimensional neutronics calculations.

collimated by the barrier shielding. There is no direct line-of-sight for neutrons from the central cell to the internal ring.

Simple one-dimensional heat transfer calculations were done using the model outlined in Fig. 7. The volumetric heating rates are estimates from the neutronics analysis and the surface heating load is 0.45 MW/m^2. The design and basis for choosing a low melting point Pb-Sn layer (to take advantage of isothermal energy absorption upon melting) are described in Ref. 29. Results of the calculations are given in Fig. 8.

TABLE III

SATYR Superconducting Internal Ring Magnet Characteristics

Magnet type	Higher order solenoid
Inside coil radius (m)	3.35
Outside coil radius (m)	4.25
Radial coil thickness (m)	0.90
Axial coil length (m)	4.00
Coil cross section (m^2)	3.60
Coil volume (m^3)	87.92
Operating temperature (K)	4.2
Overall current density (MA/m^2)	26
Magnetic field at the plasma surface outside the magnet (T)	12
Conductor type	Copper-stabilized Nb_3Sn
Structural material	Stainless steel
Volume fraction	
Nb_3Sn (%)	8
Copper stabilizer (%)	50
Liquid helium (%)	9
Insulation material (%)	33

One criterion for the maximum time before the coil must be recooled to its initial cryogenic condition is that the superconductor temperature should not exceed 12 K. It is found however that after 4 days of operation, the temperature limit of the superinsulator (T_{max} = 500 K) is reached. At temperatures above this maximum allowable temperature, the thermal conductivity will increase, leading to damage. Thus, thermal damage to the superinsulation is the most severe criteria. At 20 days, the nitrogen buffer layer has reached its boiling point, which would result in an unacceptable increase of the internal pressure of the coil. Another problem associated with the nitrogen gas is increased heat transfer due to natural convection. At 45 days, the temperature of the superconductor will have reached the design limit of 12 K.

The limiting condition for the superinsulation is reached as a result of volumetric neutron-induced heating. As such, we find no real role for a melting layer such as Pb-Sn. A more optimized design is shown in Fig. 9, which has been analyzed thermally in two dimensions. Materials with low thermal conductivity, low density (for weight reduction), and good neutron-shielding properties are used.

We find from the parametric and two-dimensional heat transfer and neutronics analysis that the shield

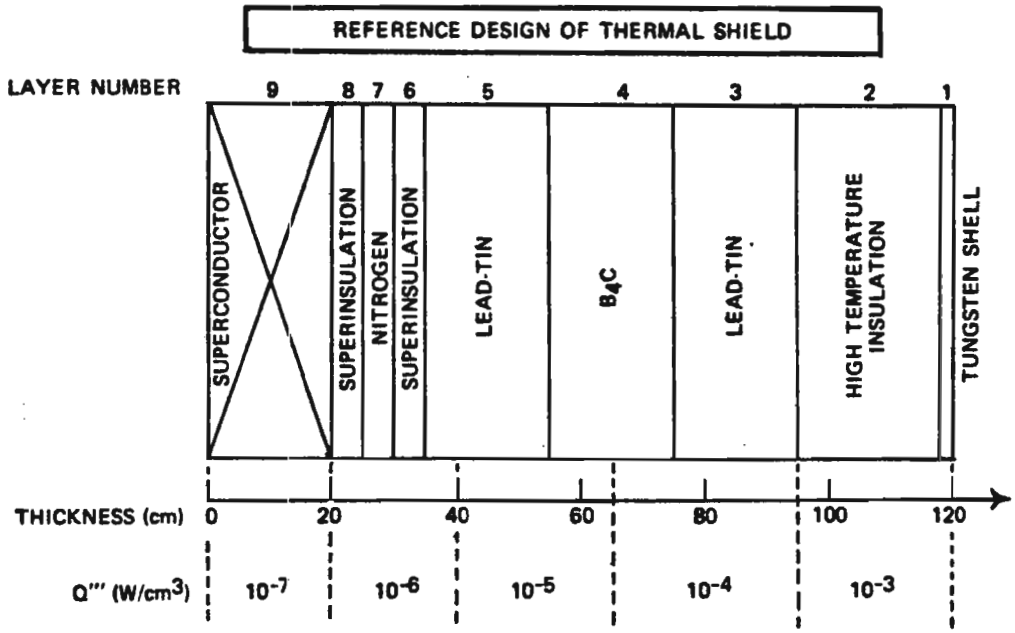

Fig. 7. Simple one-dimensional model of the internal ring and its shielding, used in parametric heat transfer calculations.

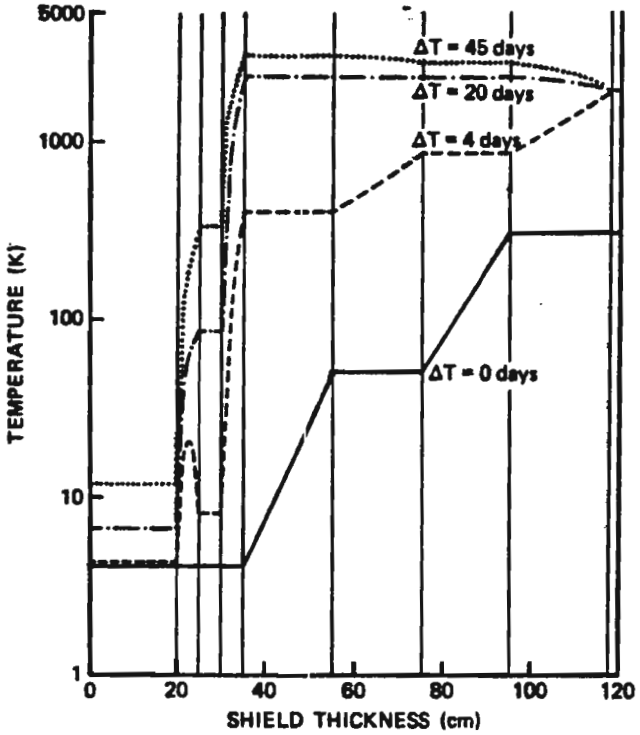

Fig. 8. Calculated temperature profile through ring thermal shield at various times after startup of the reactor.

will adequately protect the superconductor and superinsulation for a minimum of 14 days. After that, the plasma must be shut down to attach coolant feed tubes to the levitated coil, and via forced convection, cool the coil to the prescribed temperature distribution. Hence, the SATYR D-D reactor would be a pulsed device with an operating period of ~2 weeks. (True steady state is possible with this configuration only if coolant leads through the plasma to the hoop are tolerable. Such leads can be magnetically guarded but the impact on plasma $n\tau$ is quite uncertain.[30,31])

Coil levitation in a configuration such as that used for SATYR will be required regardless of whether or not coolant leads through the plasma are allowed. The reason is that the weight of the ring is so great (~2000 tonnes with shielding). In the past, plasma experiments with horizontally floating superconducting internal coils have been successful.[32,33] A simple analysis based on an extension of Earnshaw's theorem[34] can be used to show that the ring is readily supported with external coils arranged, for example, as shown in Fig. 10. Although the levitated coil in SATYR carries 94 MA, the current in the external levitating coils is only ~1% of this value.

Major issues not yet fully addressed relate to the stability of the floating hoop. If attention is restricted to systems of axial symmetry about the horizontal

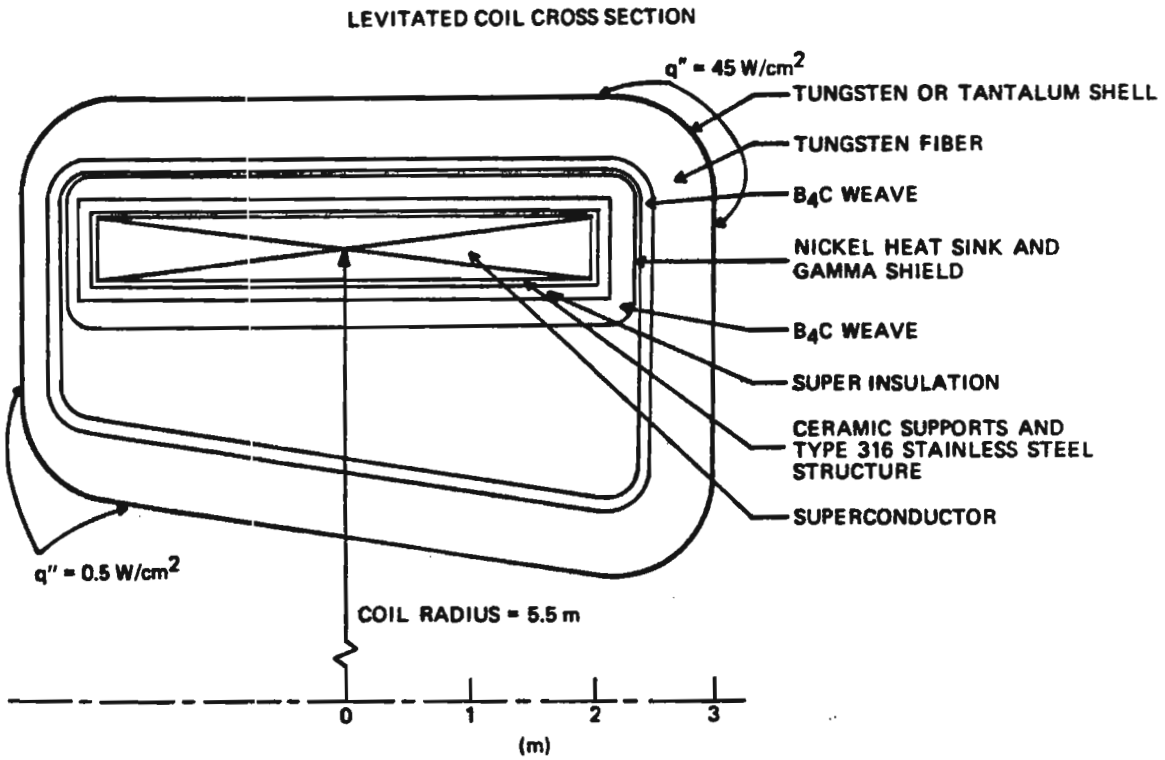

Fig. 9. Optimized internal ring shielding configuration in SATYR. Note use of low-density weaves and fibers and the absence of a heat-holding melt layer.

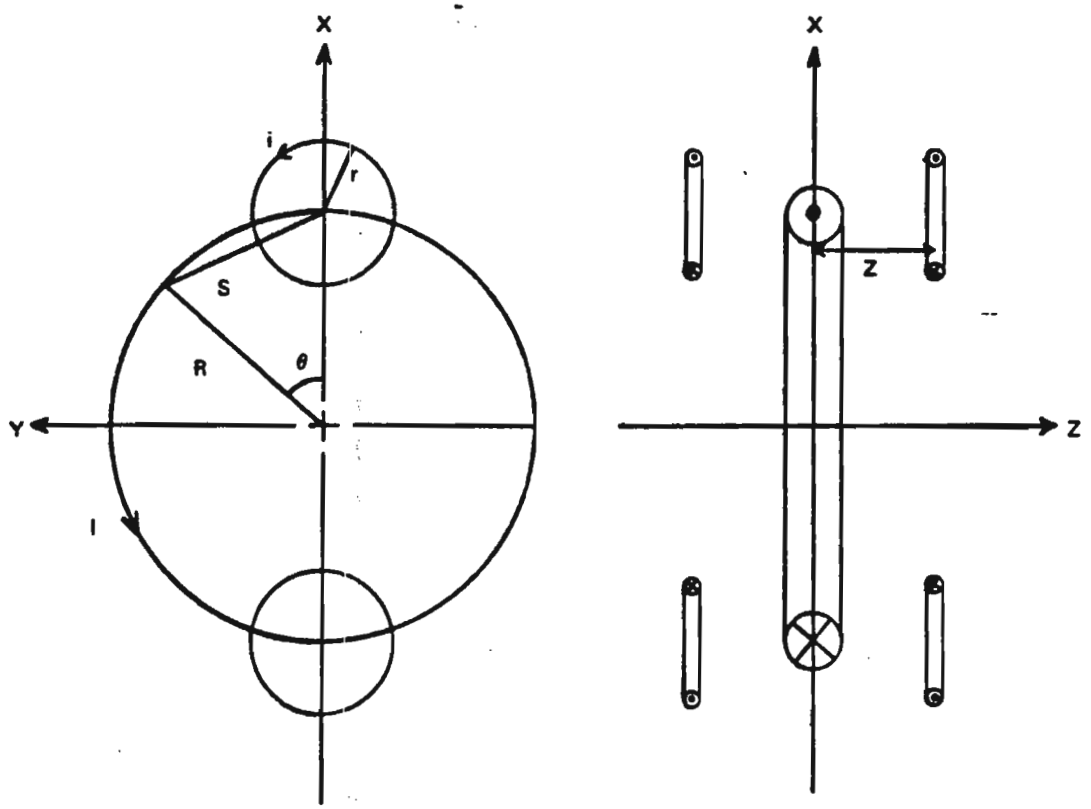

Fig. 10. External coil placements to levitate the single internal ring.

z axis, the levitated coil will be unstable to tilting, i.e., horizontal or vertical instability. Active stabilization will be necessary. In addition, the coil may rotate about the z axis. The method of stabilization to prevent this rotational motion requires a feedback coil system analogous to the one used in the Princeton FM-1 experiment.[34] An optical system will sense the rotating motion and be used to control the current in magnetic feedback coils. The current in the feedback coils, and therefore the feedback forces, will be proportional to the displacement and velocity of the main coil. The feedback control system can consist of a light source for each motion, a photocell, and associated electronic circuitry. When the light coming from the source is intercepted by the optical edge attached to the levitated coil, the feedback system reacts to supply enough current to the stabilizing coil to oppose the rotational motion. A rather detailed levitation-stability study for an octupole design has recently been completed.[35] It is an appropriate reference for an even more complicated problem of this type.

II.D. Blanket Design, Analysis, and Power Balance

We turn now to a description of the SATYR blanket concept and its associated analysis. Our aim is to use a relatively small number of high-integrity vessels rather than a large number of small-size tubes for heat removal. The unique features of D-D systems, particularly low-power density, no tritium breeding, and, in the case of mirrors, low surface heat loading leads to greater blanket design flexibility.

II.D.1. Blanket Design Philosophy

Previous reactor designs for tandem mirrors[36,37] have used either many small diameter tubes or many small "pods" for blanket breeding and heat-removal purposes. The design philosophy in SATYR is to use a relatively small number of high-integrity vessels. The aim is greater reliability. The unique features associated with D-D in a tandem mirror are used to advantage in the design. The low fusion power density compared to D-T reactors leads to lower values of radiation damage parameters and transmutation rates in the blanket structural material. Normal blanket lifetime limitations are thus relaxed. For SATYR, two basic designs are analyzed: design A, based on a sintered aluminum product (SAP) alloy with water cooling; and design B, a ferritic steel blanket with helium cooling. Design B is our preferred concept for reasons that will become clear.

A major design criterion is to achieve a blanket lifetime that is comparable to plant lifetime (~30 yr). Long-term storage of activated materials will then be

part of plant decommissioning except for statistical failures requiring blanket removal because *in situ* maintenance is not possible. However, overall blanket reliability should be increased due to fewer blanket components and the fact that we are operating for most of plant life relatively far from radiation damage limits. Considerations of component fabricability and material resources are used in our analysis to choose module materials and shapes.

The central cell module, as shown in Fig. 11, is a toroidal vessel with a circular cross section. The major and minor radii are 1.75 and 0.35 m, respectively. A section of the central cell blanket is shown in Fig. 12. The central cell is 225 m in length and consists of 320 modules. Inside each vessel is a static bed of small metal spheres. The neutron energy is multiplied and deposited in the spheres as thermal energy.

II.D.2. Blanket Neutronics and Photonics

The main objective in the SATYR central cell blanket nuclear design has been to minimize the average blanket power multiplication, M_{av}, defined as the ratio of the heat deposited in the blanket to the source neutron kinetic energy. Since there are two types of distinct neutrons emitted per D-D reaction, M_{av} is

$$M_{av} = \frac{(M_{D\text{-}T} \times 14.1) + (M_{D\text{-}D} \times 2.5)}{2 \times 8.3} ,$$

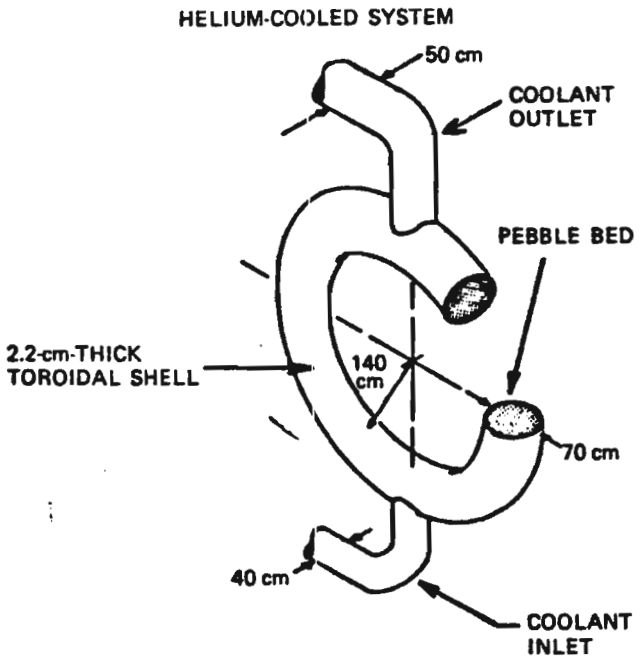

Fig. 11. Schematic picture of a single pressure-vessel-type blanket.

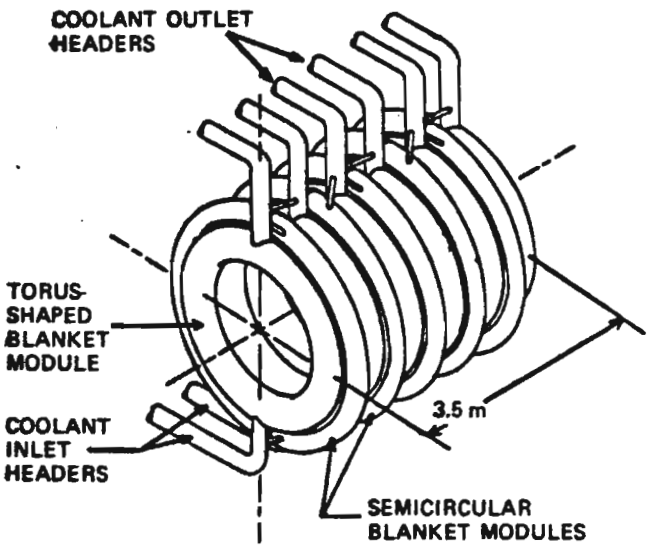

Fig. 12. Perspective view of pressure vessel blanket in the central cell of SATYR.

where the factor 8.3 is the average neutron kinetic energy per D-D reaction. The blanket power multiplication factors are $M_{D\text{-}T}$ and $M_{D\text{-}D}$ for the D-T and D-D neutron, respectively.

The design objective has been to maximize $M_{D\text{-}T}$, $M_{D\text{-}D}$, and hence, M_{av}, by enhancing the radiative neutron capture in ^{56}Fe (92% of the naturally occurring iron. The reaction Q value is 7.6 MeV.). This reaction occurs at all neutron energies. Neutrons are moderated through inelastic scattering collisions in iron and other structural materials. Carbon is used to reflect neutrons into the iron zones to further enhance the total power deposited in the blanket.

In the parametric calculations, the blanket is approximated by alternating coaxial zones of iron spheres and carbon spheres with ~60% pebble-bed packing fraction. The coolant occupies the balance of the volume. The two structural materials considered in the nuclear analysis are the ferritic steel (AISI/SAE 4130) and SAP. Boiling water is the coolant for the SAP blanket and high-pressure helium for the ferritic steel blanket.

Results are summarized in Table IV. The power multiplication for the D-T neutron, $M_{D\text{-}T}$, is 1.4 in design A. The corresponding value for the D-D neutron, $M_{D\text{-}D}$, is 4.2. Obviously, the larger multiplication for the D-D neutron is the result of having a more softened neutron spectrum in the blanket and more radiative capture events in the iron spheres. This enhanced reaction increases the gamma-ray flux in the blanket and leads to ~82% gamma-ray heating compared to the value of 69% in the D-T neutron case. The average energy deposited in the blanket per D-D reaction is 15.14 MeV, mostly due to the D-T neutron (65%). However, because of the large value

TABLE IV

Nuclear Parameters Characterizing SATYR Blanket Designs

(Total neutron wall loading is 0.4 MW/m^2.)

Parameter	Design A SAP Structure + Water Coolant			Design B Ferritic Steel Structure + Helium Coolant		
	Based on 0.4 MW/m^2			Based on 0.4 MW/m^2		
Displacements per atom in first wall (dpa/yr)	5			4		
Helium production in first wall (appm/yr)	75			27		
Hydrogen production in first wall (appm/yr)	160			115		
	D-T Neutron (14.1 MeV)	D-D Neutron (2.45 MeV)	Per D-D Reaction	D-T Neutron (14.1 MeV)	D-D Neutron (2.45 MeV)	Per D-D Reaction
Neutron heating	6.18	1.92	4.05	3.49	1.02	3.22
Gamma heating	13.53	8.63	11.1	16.18	9.5	12.19
Total nuclear heating	19.71	10.56	15.14	19.67	10.5	15.41
Energy multiplication in blanket	1.4	4.22	1.82	1.4	4.2	1.86

of the factor $M_{D\text{-}D}$, the average multiplication, M_{av}, is 1.82. Shown also in Table IV are results for design B where ferritic steel is used as structure and helium replaces water as the coolant. The resulting power level of neutron moderation means that the $^{56}Fe(n,\gamma)$ reaction rate is smaller. The average energy deposited per D-D reaction decreases from 15.14 to 15.09 MeV, a trivial adjustment.

The power density as a function of position through both designs is shown in Fig. 13. The maximum power density in either case is <6 W/cm^3, which in turn is an order of magnitude lower than those values encountered in D-T reactors.[38] Note that the power density drops by about three orders of magnitude across the water-cooled blanket while it drops by less than two orders of magnitude in the helium-cooled blanket. Therefore, the maximum-to-average power density in the helium-cooled blanket is more nearly unity. This is advantageous from a thermal-hydraulic design standpoint.

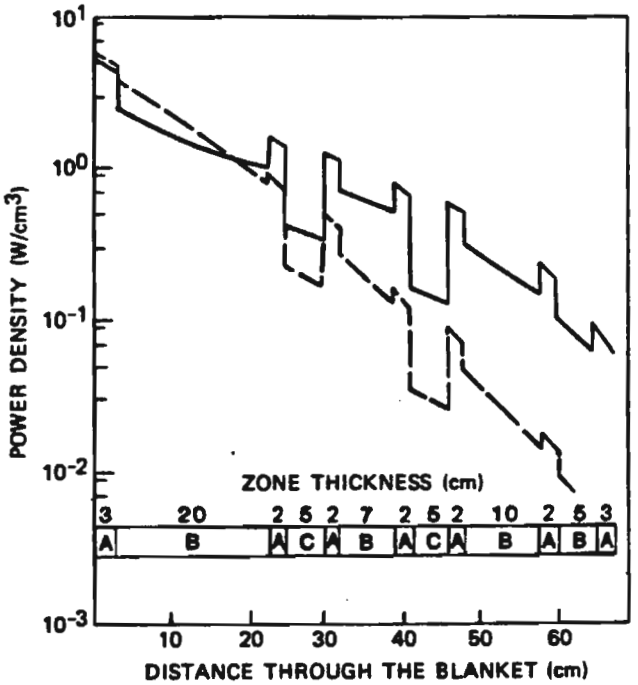

Fig. 13. Nuclear power density in the blankets of SATYR. The solid line is for design A, the dashed line for design B.

II.D.3. Thermal Hydraulics

The pebble-bed concept creates a large surface-to-volume ratio for enhanced heat transfer and provides a large mass for thermal storage in the event of a loss-of-coolant accident (LOCA). In design A, boiling water with a SAP structure, two-phase steam is used as the coolant. In actuality, subcooled

water will enter the lower header. The water will be heated to its saturation temperature in the lower portion of the blanket. After reaching the saturation temperature, the energy removed from the pebbles will result in conversion of water to steam along the middle portion of the blanket. Finally, in the upper portion, the steam will become superheated. To be precise, one must calculate the pressure drop in each of the three regions. In this work, the pressure drop was calculated using only steam along the entire blanket, a simplification that leads to a conservative estimate of the pumping power necessary to overcome the pressure drop. A bed of 1.0-cm-diam spheres will have a pressure drop of ~70 psi.

Design B, a ferritic steel structure with helium cooling, has a lower heat capacity and requires a larger mass-flow rate. Therefore, the sphere diameter must be increased to allow a decrease in the pumping power required. Using 2.5-cm-diam spheres leads to a 30-psi pressure drop. The helium circulating power is 81 MW(electric).

A summary of thermal-hydraulic parameters for the two designs is given in Table V. The net thermal efficiencies of the two designs, A and B, are 28 and 39%, respectively. The helium-cooled design achieves a significantly higher efficiency because of its capability to produce high-temperature steam. Plant power flow diagrams for the two designs are given in Figs. 14 and 15. The net plant efficiency of design A is 21% while design B is 27%. The first value is clearly unacceptable and the second is marginal. We return to this point later.

II.D.4. Material Analysis

The materials analysis for SATYR, particularly relating to the use of ferritic steels, is given in a separate paper.[39] Here, we briefly summarize major findings. The high-strength ferritic steel AISI 4130 is the primary structural alloy for the gas-cooled version of the blanket design (design B). Ferritic steels were chosen over the more commonly used austenitic steels (e.g., Types 316 and 304 stainless steel) because of their radiation damage resistance and superior thermophysical properties. The specific choice of AISI 4130 is based on minimizing long-term radioactivity. However, the lifetime analysis is generic to all chromium-molybdenum (or ferritic) steels. In particular, the conclusions of this work are not restricted to AISI 4130 but can be equally applicable

TABLE V

SATYR Blanket and Power Parameters

Total fusion power (MW)	2000	
Injected power (MW)	308	
Fusion power amplification factor, Q	6.5	
Blanket energy multiplication	1.9	
Power to direct converter (MW)	1345	
Direct converter efficiency (%)	70	
Power in thermal conversion cycle (MW)	1950	
Neutron wall load (MW/m^2)	0.43	
First-wall surface heat load (MW/m^2)	0.12	
Blanket module type	Torus-shaped vessel with an internal pebble bed	
	Design A	Design B
Structural material	SAP	AISI/SAE 4130 ferritic steel
Coolant type	Boiling water	Helium
Inlet temperature (°C)	200	370
Outlet temperature (°C)	260	520
Inlet pressure (MPa)	4.5	4.1
Pressure drop (MPa)	0.69	0.04
Mass-flow rate (kg/s)	770	1420
Thermal conversion cycle efficiency (%)	28	39
Net electric output [MW(electric)]	706	903
Net plant efficiency (%)	21	27

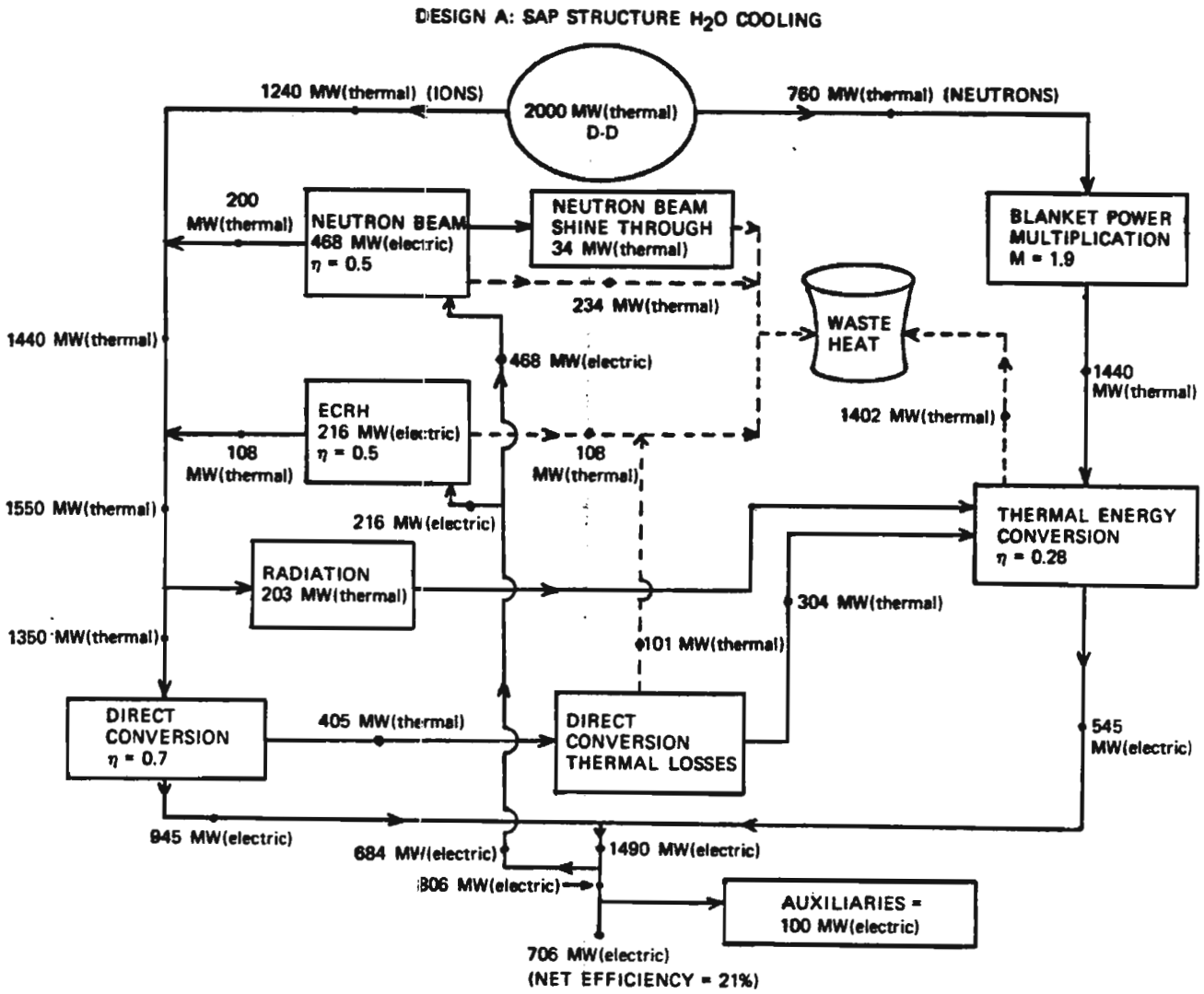

Fig. 14. Power flow diagram for SATYR with a SAP blanket and water cooling.

to other ferritic steels (HT-9; EM-12; 2¼ Cr–1 Mo, etc.).

The AISI 4130 ferritic steel is a popular steel alloy because of its good formability and weldability along with an excellent combination of mechanical properties.[40] It is a ferromagnetic material, which, like HT-9, saturates quickly in a magnetic field and can thus have minor effects on the confining magnetic fields.[41] The ultimate tensile stress (F_{tu}) is very high at room temperature, approaching 200 ksi with sufficient uniform elongation (~10%). However, at high temperatures (≳700°F), the F_{tu} decreases substantially and care must be exercised.

Creep-rupture properties of AISI 4130 are concluded to be a major lifetime determining property at high temperatures. A maximum design stress of 30 ksi can be tolerated at 500°C and 12 ksi at 560°C, if a blanket lifetime of 30 yr is to be expected. At temperatures ≲400°C, AISI 4130 is embrittled by the accumulation of radiation-induced defects. A continuous increase in the ductile-to-brittle transition temperature is a serious design concern. Thus, the inlet coolant temperature must be kept above ~400°C, or a periodic annealing procedure should be employed if inlet coolant temperatures are ~300 to 350°C. The annealing frequency is determined by the irradiation temperature and would be less frequent at higher inlet coolant temperatures. The annealing temperature should be kept ≲500°C since, at higher temperatures, temper embrittlement can be a problem. At temperatures in the range of 400 to 550°C, helium bubble swelling is predicted to be the life-limiting property.[42]

The SAP alloys, which are used with design A, have been introduced for their excellent elevated temperature creep and tensile strength. There are two main drawbacks to using SAPs: (a) low uniform elongation at elevated temperatures and (b) poor

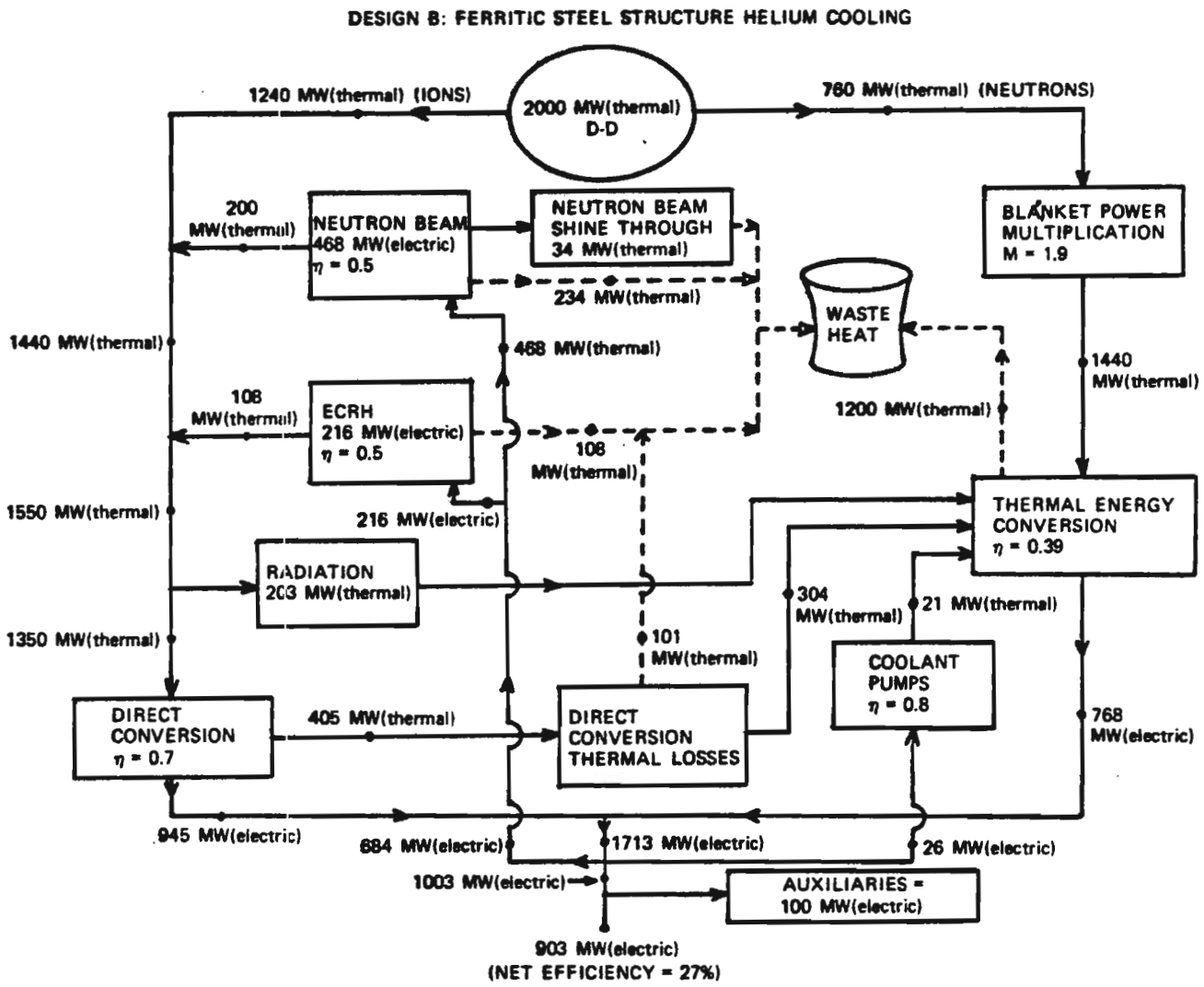

Fig. 15. Power flow diagram for SATYR with a ferritic steel, helium-cooled blanket.

fabricability and welding properties. In the SATYR design, the outlet temperature is limited to a maximum of 260°C. Newly developed welding and fabrication techniques may solve the second problem but major problems with SAP will relate to the effect of high gas concentrations on the dimensional stability of the alloy. It has been shown, however, that a more fine oxide dispersion can effectively reduce swelling by trapping gas atoms.[43]

II.D.5. Structural Analysis

For the structural analysis of the SATYR blanket module, the module is treated as a torus-shaped vessel with circular cross section containing a static bed of metal spheres. The need for high integrity and long blanket lifetime (30 yr) requires that the design stress be limited to 15 to 20 ksi due to creep-rupture problems. The general overall analysis is positive regarding 30-yr life and leads us to the view that ultimately stress concentrations, such as around a corner or near a coolant penetration, will be the life-determining factor.

An initial stress analysis is accomplished by determining the thermal and pressure stresses. The thermal stress σ_{th} is given by

$$\sigma_{th} = \frac{\pm\alpha E}{2(1-\nu)}\Delta T \ .$$

The temperature drop ΔT is given by

$$\Delta T = 1/k\left(q''t + q'''\frac{t^2}{2}\right) \ ,$$

where

α = coefficient of thermal expansion

E = Young's modulus

ν = Poisson's ratio

k = thermal conductivity

t = wall thickness

q'' = surface heat flux

q''' = volumetric heating rate.

Positive values of thermal stress (tension) are produced at the coolant/wall interface of the structure. This corresponds to the "cold" side of the vessel wall. The "hot" side, which faces the plasma, will develop compressive (negative) stresses.

The other major contribution to the total stress is the pressure-induced (or hoop) stress. The hoop stress for a thin shell is

$$\sigma_{hoop}(max) = \frac{Pr}{2t} \times \frac{2a - r}{a - r} ,$$

where

P = coolant pressure

r = torus minor radius

$a = R + r$, where R is the torus major radius.

Different combinations of the vessel coolant parameters in the stress equations have been used to determine an optimum combination for the SATYR design. A graph of total stress, σ_T, as a function of vessel wall thickness for a ferritic steel vessel is given in Fig. 16. Results are shown for three cases. The parameters used to evaluate each case are listed in Table VI. Case 1 is unacceptable due to the large stress at all thicknesses. The blanket vessel for case 2 has an acceptable stress of 16 ksi at a thickness of 0.009 m. The reduction in stress from case 1 to case 2 is due to a decrease in the minor radius from 0.35 to 0.2 m. A suitably thick blanket will require a double row of these blanket vessels. This requirement will complicate the mechanical design of the coolant manifolding. Ease of maintenance and neutron streaming will also be problems with a double row of vessels.

Case 3 has a suitable stress of 16 ksi with a 0.022-m thickness. The minor radius is 0.35 m. The reduction in stress with larger radius is a result of the

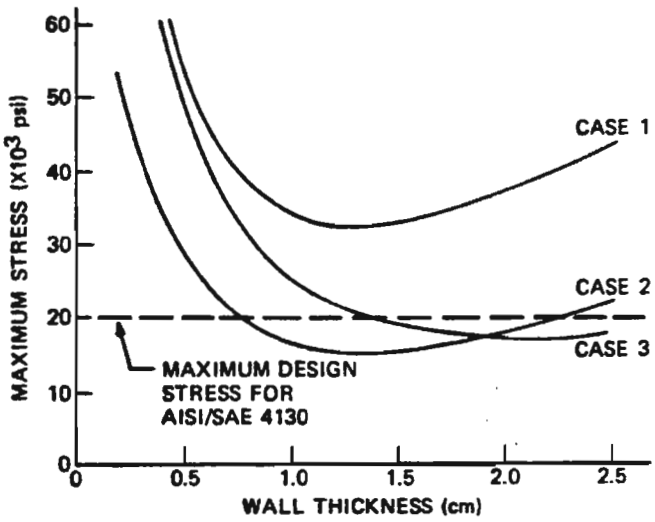

Fig. 16. Stress versus pressure vessel wall thickness for three cases outlined in text.

TABLE VI

Parameters for Blanket Vessel Stress Calculations

Structure: AISI/SAE 4130 ferritic steel
(composition–iron + 0.3% C + 0.95% Cr + 0.2% Mo)

Material properties:
Coefficient of thermal expansion, α = 1.4 (10^{-5})°C^{-1}
Young's modulus, E = 1.7 (10^5) MPa
Poisson's ratio, ν = 0.3
Thermal conductivity, k = 36 W/m·°C

Case Variations	Case 1	Case 2	Case 3
Major radius (m)	1.75	1.60	1.75
Minor radius (m)	0.35	0.20	0.35
Internal pressure (MPa)	4.1 (600 psia)	3.4 (500 psia)	4.1 (600 psia)
Volumetric heating rate (MW/m^3)	7	7	7
Surface heat flux (MW/m^2)	0.12	0.12	0
Wall thickness	Variable	Variable	Variable

addition of a curtain of small diameter coolant tubes. These tubes remove the surface heat flux striking the vessel wall. Each blanket vessel has a curtain attached to its inner surface. A cross-section view of the blanket with the first wall attached is shown in Fig. 17. A list summarizing mechanical design parameters for the two blanket designs, A (SAP plus water) and B (ferritic steel plus helium), is given in Table VII.

II.D.6. Radioactivity, Afterheat, and Biological Hazard Potential of D-D Reactors

A major reason for interest in D-D is the possibility of reducing the radioactive inventory in fusion reactors by eliminating the need to breed tritium in a blanket, by reducing the amount of tritium in the system, and by reducing the neutron-induced activity. We have studied the radioactivity characteristics

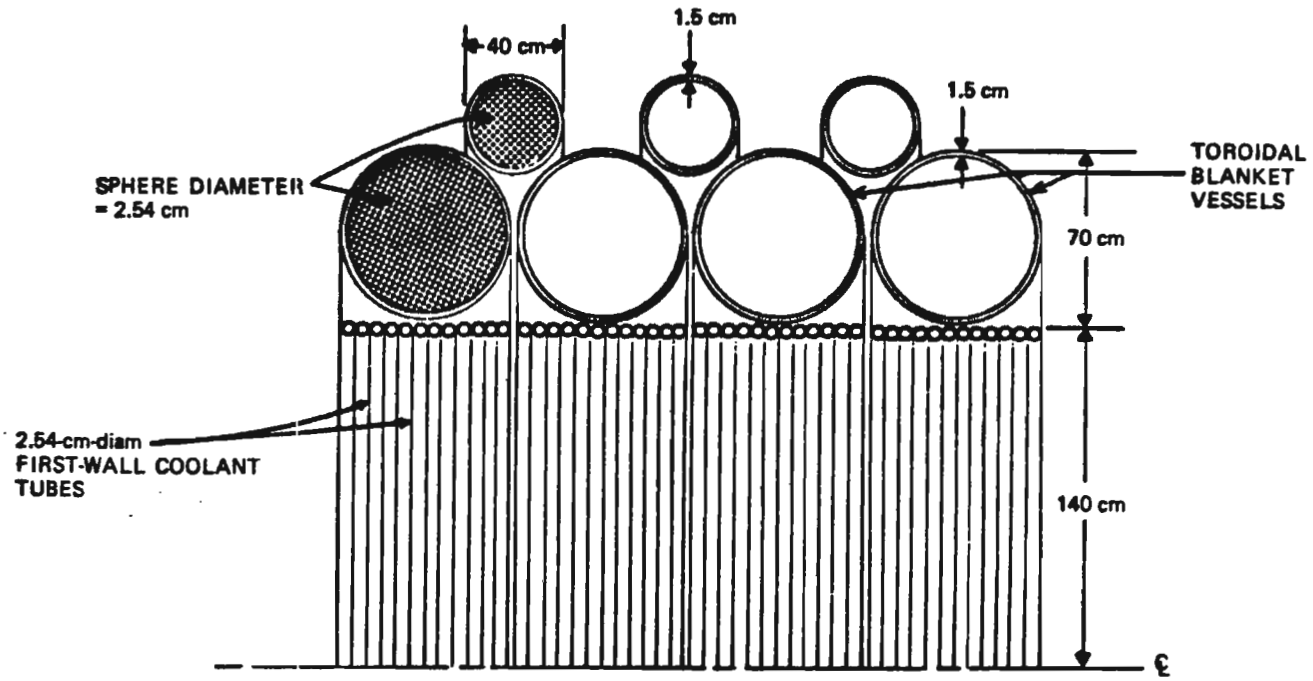

Fig. 17. Cross section of SATYR blanket showing pebble-bed pressure vessel blanket and first-wall tube bank.

TABLE VII

Blanket Module Mechanical Design Parameters

	Design A	Design B
Blanket module type	Torus-shaped vessel with an internal pebble bed	
Structural material	SAP	AISI/SAE 4130 ferritic steel
Module dimensions		
Major radius (m)	1.75	1.75
Minor radius (m)	0.35	0.35
Wall thickness (m)	0.04	0.022
Total mass of one module (tonnes)	22.7	24.2
Number of modules per blanket	320	320
First-wall type	0.0254-m-diam coolant tubes	0.0254-m-diam coolant tubes
Maximum internal pressure (MPa)	4.5 (650 psia)	4.1 (600 psia)
Maximum volumetric heating rate (MW/m^3)	7	7
Maximum stress in structure (MPa)	48 (7000 psi)	110 (16 000 psi)

of the SATYR design in detail. We summarize our findings in Sec. III where a comparison of D-D with D-T reactors is given.

The radioactivity parameters computed are expressed in terms of radioactivity per unit thermal power [Ci/W(thermal)], biological hazard potential (BHP) in units of km^3-air/kW(thermal), and afterheat per unit of operating thermal power [W/W(thermal)]. The second parameter, BHP, is defined as the amount of air (or water) required to dilute a given isotope to the maximum permissible concentration (MPC) per unit of reactor thermal power.[44] It is the activity [Ci/kW(thermal)], divided by the MPC value (Ci/km^3) of air. The MPC values used in the present study are extracted from the values listed in the U.S. Atomic Energy Commission rules, Title 10, Part 20. For isotopes not found in these rules, the MPC is calculated using the values reported by Dudziak and Krakowski.[45] The BHP is a meaningful but general parameter usable for comparison. However, the absolute value has no real significance since factors such as volatility, chemical state, source distribution, and accident scenario are not specified. The calculations were performed with the DKR radioactivity code.[46]

Nuclear afterheat levels are important since they influence both accident and long-term radwaste disposal analysis. The thermal power used is the total plant thermal power, $P_{th}(plant)$, including the power deposited in the blanket and the power extracted from the charged particles by direct conversion (~60% of the total thermal power for the D-D cycle). This must be kept in mind when comparisons are made to D-T cycle systems where the total plant thermal power is essentially only the power deposited in the blanket due to neutron interactions.

III. COMPARISON OF D-D AND D-T CYCLE REACTORS

A primary motivation of SATYR and other studies of D-D cycle reactors is the perception that they will have advantages relative to D-T cycle machines. The problem is to develop quantifiable criteria on which to make the comparison. Oft-touted advantages relate to safety (absence of lithium, absence of tritium in the blanket, absence of tritium in storage), fuel supply (only deuterium extracted from water is required), and environmental impact (lower levels of neutron-induced radioactivity, less long-term radwaste for disposal, and absence of surface or deep mining for fuel). Of course, one must assess such advantages with an eye toward the associated economic impact and then exercise reasonable judgment. The SATYR study has had a limited scope and a complete balance-of-plant (BOP) design and economic analysis (such as those carried out for WITAMIR-I, a D-T tandem mirror,[5] and STARFIRE, a conceptual D-T tokamak[11]) has not been done. However, we have completed analysis and design for a sufficient number of major subsystems (plasma, blanket and shield, magnets, plasma heating, power cycle) to quantitatively compare key parameters that are good indicators of relative merit with respect to economics and, to a degree, safety and environmental impact.

For relative economic merit, several factors are chosen. Three are related to power density, i.e., the amount of material and volume required to build the fusion part of a plant generating a given amount of power. These are: plasma power density (MW/m^3), blanket specific power density [MW(electric) per tonne of solid material in the blanket], and neutron wall loading (MW/m^2). A fourth parameter is related to the cost of the magnet system, namely, the magnetic stored energy [MJ/MW(electric)]. The final three are measures of the BOP, the system power cycle, and its efficiency; i.e., plasma Q value, recirculating power fraction (in percent), and net plant efficiency [MW(electric) to the line divided by total plant thermal power in MW(thermal)].

Safety and environmental impact scaling factors are not as easily chosen, particularly for safety issues where design is such a key factor. We have examined earlier studies of safety,[47-49] materials resource requirements,[50] and environmental impact[51] of fusion and selected parameters related to key reactor subsystems or radioactivity and radwaste disposal. The parameters selected are:

1. first-wall and blanket material inventory [tonne/MW(electric)], selected because first-wall volatility is an issue, and because it is a measure of mineral resource impact
2. first-wall specific radioactivity parameters at shutdown [$Ci/kg \cdot MW(thermal)^{-1}$], selected for the same reasons as given in item 1
3. the form of lithium, which influences safety
4. the lithium inventory in the blanket
5. tritium loss rate from the plasma to the vacuum and gas-handling systems, selected because it is a measure of the tritium in gaseous form and at greatest risk
6. blanket tritium inventory (kilograms), because this tritium is at risk in case of a blanket accident
7. tritium in storage (kilograms), the main contributor to on-site inventory
8. scheduled number of blanket replacements during plant life, a factor that influences plant availability, system reliability (including the reliability of the maintenance systems), and radwaste material levels

9. radioactivity, in the form of three parameters, i.e., specific radioactivity [Ci/kg·mW(thermal)$^{-1}$], afterheat [W/kg·MW(thermal)$^{-1}$], and BHP [km^3-air/kg·MW(thermal)$^{-1}$], given at 1000 yr after plant shutdown. This is relevant to the radwaste disposal question.

A list of economic scaling factors is given in Table VIII and the corresponding list of safety and environmental scaling factors is given in Table IX. The economic scaling factors indicate again what has been pointed out many times (see, e.g., Refs. 6 and 10), namely, that D-D cycle systems are five to ten times poorer in terms of material and volume utilization per unit power generated. Estimates of the cost of electricity from D-T cycle reactors[5,11] are 1 to 1.5 times that of existing commercial sources (coal and light water nuclear reactors). (Typical estimates show that the nuclear island in a fission reactor contributes 15 to 20% to the total cost whereas in a fusion device, the nuclear island costs are 40 to 60% of the total. Since BOP costs should be similar, the greater estimated expense of fusion machines is not surprising.) It is very likely that D-D cycle systems such as SATYR will be several factors yet more expensive. This is supported by the magnetic stored energy parameter, which is twice as large in SATYR as in the D-T reactors, despite the high value used for central cell beta.

For tandem mirrors, our analysis has shown that it will be difficult to achieve a plasma Q value much greater than 5 using the D-D cycle. In turn, this leads to a high value of recirculating power fraction and a low value of net plant efficiency, both of which point to expensive BOP and poor regional water utilization. We conclude that the economic prospects for D-D cycle reactors, if designed as modest Q, axisymmetric BTMRs, are poor and that the economic motivation to supplant D-T cycle systems is nil.

Comparison of the safety and environmental impact parameters suggests various things. The first-wall and blanket material inventory is about six times larger for the D-D system but the number of blanket replacements is five for the D-T reactors and zero for SATYR. As such, the total blanket material required over the plant lifetime is about the same. We conclude that, except for lithium, the impact on mineral resource requirements will be about the same. (For an analysis of D-T cycle reactor mineral resource requirements, see Ref. 50).

The first-wall specific radioactivity at shutdown is a factor of 10 lower in SATYR than, e.g., in STARFIRE and, of course, there is no lithium or tritium in the SATYR blanket. There is, however, six times as much total material in SATYR for a given level of power output. Also, the lithium can be in ceramic form in D-T reactors. Nevertheless, the first-wall afterheat power density is a key determinant of the ability to vaporize material in an accident, and we conclude from the numbers in Table IX that it will be significantly lower in SATYR. Thus, we conclude that the low radioactivity power density and the absence of both lithium and tritium in D-D systems are clear potential advantages.

Likewise, there appears to be a substantial advantage to D-D reactors with respect to the amount of tritium one might consider to be vulnerable to release or, in other words, at risk. Taking the plasma tritium leakage rate to the vacuum system as a measure of the tritium content in that system, we find this rate to be 20 to 40 times lower in SATYR than in the D-T reactors. The blanket tritium inventory is nil relative to D-T reactors, as is the amount of tritium in on-site storage. The conclusion that

TABLE VIII

Economic Impact Scaling Factors

	SATYR Design B (D-D, Ferritic Steel Structure)	WITAMIR-I[a] (D-T, Ferritic Steel Structure)	STARFIRE[b] (D-T, PCA[c] Structure)
1. Plasma power density (MW/m^3)	2.2	11.3	4.5
2. Blanket specific power density [MW(electric)/tonne]	0.11	1.4	1.0
3. Neutron wall loading (MW/m^2)	0.4	2.4	3.6
4. Magnetic stored energy [MJ/MW(electric)]	90	42	51
5. Plasma Q value	6.5	28	39
6. Recirculating power fraction (%)	47	18	13
7. Net plant efficiency (%)	27	40	30

[a]From Ref. 5.
[b]From Ref. 11.
[c]An advanced stainless steel.

TABLE IX

Safety and Environmental Impact Scaling Factors

Parameter	SATYR Design B D-D Cycle, Ferritic Steel Structure, Helium Coolant	WITAMIR-I[a] D-T Cycle, Ferritic Steel Structure, LiPb Coolant	STARFIRE[b] D-T Cycle, PCA Structure, Water Coolant
1. First wall and blanket weight			
a. Structure	3.4	3.5[c]	0.37
b. Solid or liquid filler	5.6[d]	5.4[e]	0.92[f]
2. First wall and blanket specific radioactivity parameters at shutdown			
a. Radioactivity [Ci/W(thermal)]	1.1	0.7	1.5
b. BHP [km^3-air/kW(thermal)]	5.1×10^{2}	4.5×10^{1}	4.23×10^{3}
c. Afterheat [W/W(thermal)]	5.5×10^{-3}	7×10^{-3}	3.1×10^{-2}
3. Form of lithium	---	Liquid; $Li_{17}Pb_{83}$	Ceramic; $LiAlO_2$
4. Lithium inventory [tonne/MW(electric)]	---	0.052	0.053
5. Tritium loss rate from the plasma to the vacuum system [kg·s^{-1}/MW(electric)]	3.7×10^{-10}	1.3×10^{-8}	7.3×10^{-9}
6. Tritium inventory in blanket breeder [kg/MW(electric)]	---	6.6×10^{-5}	8.3×10^{-3}
7. Tritium in storage [kg/MW(electric)]	---	1.4×10^{-3}	8.9×10^{-4}
8. Scheduled number of blanket replacements during plant life	0	5	5
9. Blanket radioactivity parameters at 1000 yr after plant shutdown			
a. Radioactivity [Ci/W(thermal)]	3.3×10^{-6}	2.5×10^{-5}	1.86×10^{-5}
b. BHP [km^3-air/kW(thermal)]	1.5×10^{-2}	4.5×10^{-3}	3.5×10^{-3}
c. Afterheat [W/W(thermal)]	9.7×10^{-10}	3.0×10^{-9}	1.6×10^{-8}

[a]From Ref. 5.
[b]From Ref. 11.
[c]Large because a solid ferritic steel reflector is used in the blanket.
[d]Solid filler is ferritic steel balls; coolant is helium.
[e]Filler is liquid $Li_{17}Pb_{83}$, also used as the coolant.
[f]Solid fillers are lithium aluminate, the neutron multiplier, and the graphite reflectors. We have not included the weight of the water coolant.

there is a substantial reduction in the amount of tritium at risk agrees with that drawn in Ref. 10. They conclude that the vulnerable tritium content is reduced by a factor of 200 in a D-D tokamak when compared to the D-T cycle STARFIRE reactor. They also point out that, although the risk is reduced, all the tritium safety systems required in a D-T device are also needed in D-D reactors and that the cost of the fuel-reprocessing equipment is approximately the same.

Finally, we can compare radioactivity levels at long times after plant shutdown to provide an indication of relative advantage with respect to radwaste disposal. We have already noted that the long life of D-D reactor blankets is offset by the lower specific material requirements of a D-T blanket. The total amount of radwaste material at the end of plant life is essentially the same. The specific radioactivity is significantly lower in the SATYR blanket at 1000 yr after plant shutdown but the afterheat and BHP levels are (within a factor of 2 to 4) about the same. We therefore conclude that, with respect to radwaste disposal, no significant difference exists among the systems examined.

The various radioactivity indicators for both D-D and D-T cycle systems are 10^{-6} to 10^{-8} times the levels at plant shutdown. The absolute levels are ~100 times below those in fission reactors.[51] Of course, it is well known[46] that the radioactivity level in fusion reactor radwaste can be made much lower still by appropriately choosing the blanket structural and filler materials (e.g., by choosing the vanadium alloy, V–20 Ti, as the structure, and choosing filler materials such as lead, tungsten, and vanadium.) On the other hand, except for the breeder, such materials are also potentially usable in either D-D and D-T

cycle systems. So again, D-D systems present no distinct advantage regarding radwaste disposal when compared to D-T cycle reactors.

To summarize, we find that the advantages of D-D BTMRs similar to SATYR (axisymmetric systems with high β_c) are minimal relative to D-T BTMRs. The disadvantages, on the other hand, are significant, especially with respect to system economics. As a general remark,[52] the advantages of D-D cycle systems will become significant if the power density can be increased (e.g., by operating the central cell of a BTMR at higher magnetic field) to improve reactor economics and if the neutron energy can be either collected in an advanced low radwaste blanket (e.g., utilizing vanadium alloy structures filled with lead or tungsten, graphite, and water) or be essentially discarded in favor of constructing the blanket of low radwaste materials (e.g., aluminum alloys with lead, graphite, and water filler) that operate at low temperature (100 to 150°C). The burden in this last case then shifts back to the plasma physics, which must yield an open-ended configuration with high D-D cycle Q and very high end potential to permit efficient (~80%) direct conversion.[52] By contrast, the burden to produce a low radwaste D-T system lies not with plasma physics but with materials development.

IV. SUMMARY AND CONCLUSIONS

From the D-D cycle SATYR reactor study itself and from the comparisons between it and D-T cycle reactor analyses and designs, we have drawn a number of both general and specific conclusions. Results from our reactor plasma analysis strongly suggest that high values of central cell beta are crucial to finding even marginal D-D cycle BTMRs. Such a high value of β_c is most likely to be achieved with a fully axisymmetric configuration and an MHD stable barrier cell. An axisymmetric central cell is required to minimize both radial transport losses and a decrease in the plasma $n\tau$ value. The plasma operating parameters and Q value have been optimized with the constraints that the maximum central cell beta is 70% and the maximum magnetic field in the system is 15 T. If either β_c or B_{max} can be higher, then Q can be somewhat increased.

The SRFR plug-barrier configuration proposed for SATYR is axisymmetric but it needs much further investigation. In particular, there are major questions associated with the presence of on-axis nulls, both in terms of MHD stability, enhanced particle loss, and enhanced trapping of passing particles in the barrier. It seems clear that neither this design nor others that have been discussed in the literature[16] have yet uncovered the final, optimum approach. Importantly, however, our general conclusions are not affected since we have not assessed special penalties on the plug-barrier configuration.

The neutral beam and ECRH power requirements are both reasonable, although the maximum beam energy required (700 keV) is very high. For ECRH, the major questions relate to the physics description in a relativistic plasma, high-power mode filters with low loss in overmoded circular waveguides, neutron-damage-resistant windows, maximum power ratings for components, and unit costs.

The detailed studies of levitating and designing the single internal ring have shed light on coil design for any internal ring system (octupoles, dodecapoles, etc.). Levitation of a single ring is straightforward enough and can be accomplished with external windings, which carry <1% of the internal ring current. Stability of a vertical hoop is more subtle, with the ring subject to both tilting instabilities and to in-place rotation about the symmetry axis. A feedback stabilization system is required and has been discussed. Placement of the ring in the end cell, protected from line-of-sight central cell neutron bombardment, makes shielding feasible, although the coil becomes quite heavy (2000 tonnes). A detailed two-dimensional heat transfer analysis including both surface and volumetric heating shows that the time-limiting temperature increase in the coil occurs in the superinsulation, rather than the superconductor. A phase-change melt-layer of large thermal capacity is not found to be helpful (although it has been used in many previous studies) nor is a liquid nitrogen layer. For the conditions in SATYR, such a coil could operate for ~14 days before it must be recooled to its initial cryogenic condition. A major issue will be the design of the ducting inside the coil to facilitate rapid recooling of such a multilayer system.

Blanket design for D-D cycle reactors involves greater flexibility than when tritium breeding and lithium (or its compounds) are required. For SATYR, the pebble-bed blanket employing a pressure-vessel-type container has two distinct advantages: a large surface area is available for heat transfer implying a low coolant mass flow rate and the large thermal capacity of the blanket combined with the inherently low D-D reactor power density provides an increased safety margin in the event of a LOCA.

The very low blanket surface heat loading in BTMRs generally, and in SATYR in particular, is readily handled with an actively cooled first-wall tube bank. The stress level in the larger pressure-vessel-type blanket containers is then low (<20 ksi) and blanket life (limited by creep rupture) is predicted to exceed 30 yr. Combined with the relatively small number of modules themselves and inherent modularity of linear BTMRs, the blankets should have high reliability and maintenance should be simplified. The final design configuration includes iron pebbles contained in a ferritic steel pressure

vessel cooled with helium. The relatively high coolant outlet temperature of 530°C yields an acceptable 39% gross thermal cycle efficiency. A key problem in the use of ferritic steels is the need to maintain a sufficiently high *minimum* temperature to avoid a ductile-to-brittle transition. Thus a relatively narrow 200°C operating window appears to exist for use of these materials in fusion devices.

Unfortunately, the inherently low reactivity of the D-D cycle as compared to D-T leads inevitably to low Q ($\lesssim 6$), high magnetic field, and physically large BTMR systems. The low Q value is not sufficiently offset by direct conversion of the charged reaction product energy. For SATYR, the overall net plant efficiency is just 27%. And this value is obtained only by incorporating some ambitious physics parameters (such as $\beta_c = 60\%$) in the baseline of the design.

Finally, to make the consequences of our findings clearer, we have compared the D-D-based SATYR design with both a D-T BTMR and a D-T tokamak. We have considered scaling factors relating to system economics, safety, and environmental impact. As an overall summary of our conclusions, we find that while there are selected advantages to D-D cycle BTMR systems (such as blanket lifetime predictions that exceed plant life), the clear economic disadvantages and additional physics and plasma-support-technology requirements (beam energy and field strength in particular) are by far offsetting. Furthermore, while the low-power density and neutron wall loading means that D-D reactor blankets have long life and low specific radioactivity, the larger material inventory offsets these factors, i.e., both D-D and D-T systems require about the same amount of mineral resources per unit power generated and must dispose of about the same amount of solid radwaste. The safety advantage of low-power density could of course be obtained in D-T systems by making them larger (an approach rejected because of the clear economic disadvantages thereby incurred, as noted previously). We conclude that the linearity of tandem mirrors, their inherent modularity and potential for steady-state operation, their predicted high-power density and high Q value, combined with the findings of this study, suggest that optimized D-T cycle BTMRs with axisymmetry and high β_c have the potential to be economic reactor systems and should remain the major goal of mirror fusion research.

ACKNOWLEDGMENTS

Many discussions with the LAMEX research team of A. Y. Wong and with the University of California, Los Angeles, theory group are gratefully acknowledged. These discussions were an important part of the concept development represented in our work.

The research is supported by U.S. Department of Energy contract DE-AT03-80-ER52061.

REFERENCES

1. D. E. BALDWIN and B. G. LOGAN, *Phys. Rev. Lett.*, **43**, 1318 (1979).

2. B. G. LOGAN et al., *Proc. 8th Int. Conf. Plasma Physics and Controlled Nuclear Fusion Research*, Brussels, Belgium, July 1-10, 1980, CONF-800701, IAEA-CN-38/EZ, International Atomic Energy Agency (1980).

3. G. A. CARLSON et al., UCRL-52836, Lawrence Livermore National Laboratory (1979).

4. J. F. SANTARIUS and R. W. CONN, UWFDM-340, University of Wisconsin (1980); see also *Bull. Am. Phys. Soc.*, **24**, 930 (1979).

5. B. BADGER et al., "WITAMIR-I, A Tandem Mirror Reactor Study," UWFDM-400, University of Wisconsin (1980).

6. G. H. MILEY, *Fusion Energy Conversion*, American Nuclear Society, La Grange Park, Illinois (1976).

7. R. W. CONN, "Magnetic Fusion Reactors," *Fusion*, Vol. I, Part B, p. 193, E. TELLER, Ed., Academic Press, Inc., New York (1981).

8. G. H. MILEY, "Potential and Status of Alternate-Fuel Fusion," *Proc. 4th Topl. Mtg. Technology of Controlled Nuclear Fusion*, King of Prussia, Pennsylvania, October 14-17, 1980, CONF-801011, Vol. II, p. 905, National Technical Information Service (1981).

9. R. W. CONN et al., "SATYR, Studies of a D-D Fueled Axisymmetric Tandem Mirror Reactor," PPG-576, University of California, Los Angeles (1981).

10. K. E. EVANS, Jr. et al., "D-D Tokamak Reactor Studies," ANL/FPP/TM/138, Argonne National Laboratory (1980).

11. C. C. BAKER et al., "STARFIRE, A Commercial Tokamak Power Plant Design," ANL/FPP-80-1, Argonne National Laboratory (1980); see also C. C. BAKER et al., *Nucl. Eng. Des.*, **63**, 199 (1981).

12. T. B. KAISER, *Bull. Am. Phys. Soc.*, **24**, 1061 (1979).

13. W. M. TANG and P. J. CATTO, "Kinetic Effects on Ballooning Modes in Mirror Machines," SAI-254-80-594-LJ, Science Applications, Inc. (1980).

14. D. D. RYUTOV and G. V. STUPAKOV, *Dok 1 Akad. Nauk. SSSR 240*, p. 1086 (1978); see also G. V. STUPAKOV, Institute of Nuclear Physics Preprint 78-93, USSR Academy of Sciences, Siberian Branch, Novosibirsk (1978).

15. J. KESNER et al., "A Tandem Mirror with Axisymmetric Central Cell Ion Confinement," PFC/JA-81-11, Massachusetts Institute of Technology Plasma Fusion Center (1981).

16. B. G. LOGAN, *Comm. Plas. Phys. Cont. Fusion*, **5**, 271 (1980).

17. A. Y. WONG et al., "Large-Mirror-Ratio Axisymmetric Mirrors Stabilized by Surface Magnetic Fields," *Proc. Int. Symp. Physics in Open-Ended Systems*, University of Tsukuba, Japan, April 1980; see also *Bull. Am. Phys. Soc.*, **25**, 858 (1980).

18. D. L. MAMAS et al., *Phys. Rev. Lett.*, **41**, 29 (1978).

19. G. W. SHUY, Y. C. LEE, and F. KANTROWITZ, "A Stabilized Axisymmetric Tandem Mirror Plug and Barrier Using Field Reversal," PPG-523, University of California, Los Angeles (1980); see also *Comm. Plas. Phys. Cont. Fusion*, **6**, 155 (1981).

20. A. Y. WONG, University of California, Los Angeles, Private Communication (1980).

21. R. W. SCHUMACHER, *Bull. Am. Phys. Soc.*, **23**, 887 (1978).

22. S. HORTON and S. YOSHIKAWA, *Bull. Am. Phys. Soc.*, **23**, 828 (1978).

23. B. G. LOGAN, Lawrence Livermore National Laboratory, Private Communication (1981).

24. J. KESNER, *Nucl. Fusion*, **20**, 557 (1980).

25. J. KESNER, *Nucl. Fusion*, **21**, 97 (1981).

26. D. E. BALDWIN, B. McNAMARA, and P. WILLMAN, "Ideal Ballooning Modes in Axisymmetric Mirror Machines," UCID-18809, Lawrence Livermore National Laboratory (1980).

27. G. W. SHUY, "Advanced Fusion Fuel Cycles and Fusion Reaction Kinetics," PhD Thesis, University of Wisconsin (1980).

28. I. B. BERSTEIN and D. C. BAXTER, *Phys. Fluids*, **24**, 108 (1981).

29. R. W. CONN, D. ARNUSH, J. DAWSON, D. W. KERST, and V. VANEK, "Aspects of Octopoles as Advanced Fuel Cycle Fusion Reactors," *Proc. Tech. Comte. Mtg. and Workshop on Fusion Reactor Design Concepts*, p. 721, International Atomic Energy Agency (1978).

30. B. LEHNERT, *Plasma Phys.*, **17**, 501 (1975).

31. R. SCHUMACHER and A. Y. WONG, Dodecapole Experiment, University of California, Los Angeles, Private Communication (1981).

32. J. W. WILLARD, J. FILE, and G. D. MARTIN, *IEEE Trans.*, **NS-18**, 283 (1971).

33. C. E. TAYLOR and T. J. DUFFY, "Coils for the Superconducting Levitron," *Proc. 2nd Symp. Engineering Problems of Fusion Research*, Los Alamos, New Mexico, April 8-11, 1969, Institute of Electrical and Electronics Engineers (1969).

34. J. FILE et al., "Princeton Floating Multipole Superconducting Ring Progress," MATT-657, Princeton Plasma Physics Laboratory (1968).

35. J. GORDON et al., "p-^{11}B Multipole Evaluation," *Proc. IAEA Tech. Cmte. Mtg. and Workshop on Fusion Reactor Design and Technology*, Tokyo, Japan, October 5-16, 1981 (to be published).

36. G. A. CARLSON et al., "Tandem Mirror Reactors with Thermal Barriers," UCRL-52836, Lawrence Livermore National Laboratory (1979).

37. D. K. SZE and I. N. SVIATOSLAVSKY, "Thermal and Mechanical Design of WITAMIR-I Blanket," UWFDM-377, University of Wisconsin (1980).

38. E. T. CHENG, C. W. MAYNARD, W. F. VOGELSAND, and A. C. KLEIN, "Nucleonic Design for a Compact Tokamak Fusion Reactor Blanket and Shield," *Nucl. Technol.*, **45**, 77 (1979).

39. N. M. GHONIEM and R. W. CONN, "Assessment of Chromium-Molybdenum Steels for Application in Steady-State Fusion Devices," *Proc. IAEA Tech. Cmte. Mtg. and Workshop on Fusion Reactor Design and Technology*, Tokyo, Japan, October 5-16, 1981 (to be published).

40. "Aerospace Structural Metals Handbook," Department of Defense Mechanical Properties Data Center, Battelle-Columbus Laboratory (1980).

41. J. M. RAWLS et al., "Assessment of Martensitic Steels as Structural Materials in Magnetic Fusion Devices," GA-A15749, General Atomic Company (1980).

42. M. TAKATA and N. M. GHONIEM, "Intragranular Helium Gas Behavior in Fusion Reactor Structural Materials," Plasma Physics and Fusion Engineering Report PPG-519, University of California, Los Angeles (1980).

43. K. R. GARR and A. G. PARD, *J. Nucl. Mater.*, **85 & 86**, 919 (1980).

44. W. F. VOGELSANG, "Radioactivity and Associated Problems in Thermonuclear Reactors," *Proc. 2nd ANS Topl. Mtg. Technology of Controlled Nuclear Fusion*, Richland, Washington, September 21-23, 1976, CONF-760935 (1976).

45. D. J. DUDZIAK and R. A. KRAKOWSKI, "Radioactivity Induced in a Theta-Pinch Fusion Reactor," *Nucl. Technol.*, **25**, 32 (1975).

46. T. Y. SUNG and W. F. VOGELSANG, "DKR: A Radioactivity Calculation Code for Fusion Reactors," UWFDM-170, University of Wisconsin (Sep. 1976); see also RSIC Collection CCC-323, Oak Ridge National Laboratory, Radiation Shielding Information Center.

47. D. OKRENT et al., *Nucl. Eng. Des.*, **39**, 215 (1976).

48. M. S. KAZIMI and R. W. SAWDYE, *J. Fusion Energy*, **1**, 87 (1981).

49. J. P. HOLDREN, "Contribution of Activation Products to Fusion Accident Risk: Part 1. A Preliminary Investigation," *Nucl. Technol./Fusion*, 1, 79 (1981).

50. E. CAMERON, R. W. CONN, G. L. KULCINSKI, and I. N. SVIATOSLAVSKY, "Minerals Resource Implications of a Tokamak Reactor Economy," UWFDM-313, University of Wisconsin (1979).

51. W. HAFELE, J. HOLDREN, G. KESSLER, and G. L. KULCINSKI, "Fission and Fusion Breeder Reactors," RR-77-8, International Institute for Applied Systems Analysis, Austria (1977).

52. T. K. FOWLER, Lawrence Livermore National Laboratory, Private Communication (Sep. 1981). Fowler and others at LLNL have noted that the ideal D-D system is one of high Q which converts the 62% of the energy released in charged particles in an efficient (~80%) direct converter and (perhaps) discards the neutron energy (38%) in favor of a low radwaste, low activation blanket; see also B. G. LOGAN, A. A. MIRIN, M. E. RENSINK, and T. K. FOWLER, *Fiz. Plazmy*, 4, 542 (1978).